Journal of Ethnopharmacology 337 (2025) 118866

Contents lists available at ScienceDirect

Journal of Ethnopharmacology

journal homepage: www.elsevier.com/locate/jethpharm

Insights into the bioactive potential of the Amazonian species Acmella oleracea leaves extract: A focus on wound healing applications

Júlia Bertolini Fajardo [a], Mariana Hauck Vianna [a], Ana Barbara Polo [a], Mariane Rocha Cordeiro Comitre [a], Débora Almeida de Oliveira [a], Thayná Gomes Ferreira [a], Ari Sérgio de Oliveira Lemos [a], Thalita de Freitas Souza [a], Lara Melo Campos [a], Priscila de Lima Paula [a], Alan Franco Barbosa [b], Mário Geraldo de Carvalho [c], Maria Clara Machado Resende Guedes [d], Elaine Soares Coimbra [d], Gilson da Costa Macedo [d], Guilherme Diniz Tavares [e], Thaís Nogueira Barradas [f], Rodrigo Luiz Fabri [a,*]

[a] Laboratory of Bioactive Natural Products, Department of Biochemistry, Institute of Biological Sciences, Federal University of Juiz de Fora, Juiz de Fora, Minas Gerais, Brazil

[b] Federal Institute of Education, Science and Technology of Mato Grosso, Sorriso, MG, Brazil

[c] Department of Chemistry, Institute of Exact Sciences, Federal Rural University of Rio de Janeiro, Seropédica, RJ, Brazil

[d] Department of Parasitology, Microbiology, and Immunology, Institute of Biological Sciences, Federal University of Juiz de Fora, Juiz de Fora, Minas Gerais, Brazil

[e] Faculty of Pharmacy, Federal University of Juiz de Fora, Juiz de Fora, Minas Gerais, Brazil

[f] Faculty of Pharmacy, Federal University of Rio de Janeiro, Rio de Janeiro, Brazil

ARTICLE INFO

Keywords:
Acmella oleracea
Wound healing
Amazonian species
Medicinal plants
Skin wounds

ABSTRACT

Ethnopharmacological relevance: *Acmella oleracea* is traditionally used by Amazonian folks to treat skin and mucous wounds, influenza, cough, toothache, bacterial and fungal infections. Its phytoconstituents, such as alkylamides, phenolic compounds, and terpenes, are reported to produce therapeutic effects, which justify the medicinal use of *A. oleracea* extracts. However, the scientific evidence supporting the application *A. oleracea* bioactive products for wound treatment of remains unexplored so far.

Objective: This work aimed to characterize the phytochemical composition of methanolic extract of *A. oleracea* leaves (AOM) and to investigate their antioxidant, anti-inflammatory, antimicrobial and healing potential focusing on its application for wound healing.

Material and methods: The dried leaves from *A. oleracea* submitted to static maceration in methanol for 40 days. The phytochemical constitution of AOM was analyzed based on the total phenolic dosage method and by UFLC-QTOF-MS analysis. Antioxidant activity was assessed by DPPH and NO scavenging activities, as well as MDA formation, evaluation of ROS levels, and phosphomolybdenum assays. *In vitro* anti-inflammatory activities were assessed by reduction of NO, IL-6, and TNF-α production and accumulation of LDs in peritoneal macrophages cells. Antimicrobial activity was evaluated by determining MIC and MBC/MFC values against *P. aeruginosa*, *E. coli*, *S. epidermidis*, *S. aureus* and *C. albicans*, bacterial killing assay, and biofilm adhesion assessment. *In vitro* wound healing activity was determined by means of the scratch assay with L929 fibroblasts.

Results: Vanillic acid, quercetin, and seven other alkamides, including spilanthol, were detected in the UFLC-QTOF-MS spectrum of AOM. Regarding the biocompatibility, AOM did not induce cytotoxicity in L929 fibroblasts and murine macrophages. The strong anti-inflammatory activity was evidenced by the fact that AOM reduced the cellular production of inflammatory mediators IL-6, TNF-α, NO, and LDs in macrophages by 100%, 96.66 ± 1.95%, 99.21 ± 3.82%, and 67.51 ± 0.72%, respectively. The antioxidant effects were confirmed, since AOM showed IC_{50} values of 44.50 ± 4.46 and 127.60 ± 14.42 μg/mL in the DPPH and NO radical inhibition assays, respectively. Additionally, AOM phosphomolybdenium reducing power was 63.56 ± 13.01 (RAA% of quercetin) and 104.01 ± 21.29 (RAA% of rutin). Finally, in the MDA quantification assay, AOM showed 63,69 ±

* Corresponding author. Bioactive Natural Products Laboratory, Department of Biochemistry, Biological Sciences Institute, Federal University of Juiz de Fora, Juiz de Fora, Minas Gerais, CEP 36036, Brazil.

E-mail address: rodrigo.fabri@ufjf.br (R.L. Fabri).

https://doi.org/10.1016/j.jep.2024.118866
Received 26 June 2024; Received in revised form 26 August 2024; Accepted 27 September 2024
Available online 30 September 2024

3.47% of lipid peroxidation inhibition. It was also observed that the production of ROS decreased by 69.03 ± 3.85%. The MIC values of AOM ranged from 1000 to 125 μg/mL. Adhesion of *S. aureus, P. Aeruginosa,* and mixed biofilms was significantly reduced by 44.71 ± 4.44%, 95.50 ± 6.37 %, and 51.83 ± 1.50%, respectively. AOM also significantly inhibited the growth of *S. aureus* (77.17 ± 1.50 %) and *P. aeruginosa* (62.36 ± 1.01%). Furthermore, AOM significantly enhanced the *in vitro* migration of L929 fibroblasts by 97.86 ± 0.82% compared to the control ($P < 0.05$).

Conclusions: This study is the first to report total antioxidant capacity and intracellular LD reduction by AOM. The results clearly demonstrated that AOM exerts potent anti-inflammatory, antioxidant, antimicrobial, and wound healing effects, encouraging its further investigation and promising application in wound treatment.

Abbreviation list:

AOM - Methanolic extract of *A. oleracea* leaves
BHT - Butylated hydroxytoluene
COX-2 - cyclooxygenase-2
DMEM - Dulbecco's Modified Eagle Medium
DMSO - Dimethyl sulfoxide
DPPH - 2,2-diphenyl-1-picrylhydrazyl
ECM - extracellular matrix
ELISA - Enzyme-Linked Immunosorbent Assay
H2DCFDA - 2′,7′-dichlorodihydrofluorescein diacetate
IC50 - Inhibitory concentration of 50%
IFMT - Federal Institute of Education Science and Technology of Mato Grosso
iNOS - Inducible nitric oxide synthase
LDs - Lipid droplets
LPS - Lipopolysaccharide
MBC - Minimum bactericidal concentration
MDA - Malondialdehyde
MeOH - methanol
MFC - Minimum fungicidal concentration
MH - Mueller Hinton
MIC - Minimum inhibitory concentration
MMP – Metalloproteinases
MTT - 3-(4,5-dimethyl-2-thiazolyl)-2, 5-diphenyl-2H-tetrazolium bromide
NO - Nitric oxide
NSAIDS - Non-steroidal anti-inflammatory drugs
PBS - Phosphate buffered saline
RAA% - Relative Antioxidant Activity
ROS - Reactive oxygen species
SB - Sabouraud
SFB - Fetal bovine serum
SNP - Sodium nitroprusside
TAE - Tannic acid equivalent
TBA - Thiobarbituric acid
TPC - Total phenolic content
UFLC-QTOF-MS - Ultra-fast liquid chromatography-Quadrupole time of flight mass spectrometry

1. Introduction

Skin wounds are considered a growing global public concern and demand ever increasing resources from healthcare systems. Acute and chronicle wounds not only affects individual productivity, but also affects one's self-esteem, mental and clinical health, individual autonomy and social interaction (Maver et al., 2015). The rising trend in difficult-to-heal wounds is linked to the population aging, increased prevalence of chronic disease, as well as the occurrence of burns and traumatic injuries (Grand View Research, 2023).

Once the skin damaged takes place, skin barrier function must be restored immediately to maintain homeostasis (Dehdashtian et al., 2018). Therefore, wound healing comprises a dynamic, intricate and complex combination of biological processes, with an initial phase of intense inflammation, followed by a proliferative phase characterized by cell proliferation, extracellular matrix deposition and wound retraction. The third and final phase of wound healing is characterized by tissue remodeling, where previously activated processes are silenced and functional tissue formation is observed (Cañedo-Dorantes and Cañedo-Ayala, 2019; Petkovic et al., 2021). However, wound healing can be delayed by pro-inflammatory oxidative stress and microbial infection, potentially leading to impaired healing and chronic inflammation (Visha and Karunagaran, 2019).

Pharmacological treatments based on antibiotics and non-steroidal anti-inflammatory drugs (NSAIDs), are frequently used to decrease healing time and minimize unwanted complications, like scarring and infections (Maver et al., 2015). Nevertheless, prolonged use of NSAIDs impairs the healing process by reducing keratinization, epithelialization and angiogenesis. Additionally, the extended use of antibiotics can also lead to microbial resistance, hypersensitivity reactions, and contact dermatitis (Gushiken et al., 2021; Shukla et al., 2019). In this context, bioactive natural products with widespread and long-therm traditional use have been investigated as an alternative to synthetic therapeutic molecules with reduced side effects due to their mild toxicological risks and remarkable multi-therapeutic benefits.

Acmella oleracea (L.) R.K. Jansen, also known in Brazil as Jambu, Agrião do Pará and Agrião Bravo, is a plant species native to the Amazon region with known valuable nutritional and bioactive potential (Gilbert and Favoreto, 2010; Lalthanpuii et al., 2018). Jambu belongs to the Asteraceae family, whose leaves and flowers are used to prepare traditional northern Brazilian dishes such as "tacacá" and "pato no tucupi" (Uthpala and Navaratne, 2021). Jambu is often grown and commercialized by small farmers, being considered socio-economically important to the northern region of Brazil (Silva et al., 2023).

Many human diseases have been treated with *A. oleracea* in ethnomedicine. The decoction of its flowers and leaves is used to the local management of wounds, as well as influenza, cough, toothache, tuberculosis, malaria, bacterial, and fungal infections (Araújo et al., 2021; Bellumori et al., 2022; Lalthanpuii et al., 2018). The pharmacological potential of Jambu is attributed to the presence of bioactive compounds that act alone or in synergy to induce physiological responses. The aerial parts of *A. oleracea* are rich in alkylamides, particularly spilanthol, which is responsible for the sensory properties of tingling and anesthesia (Lalthanpuii et al., 2018; Savic et al., 2021). According to Bakondi et al. (2019), spilanthol is able to inhibit the expression of cyclooxygenase-2 (COX-2) and the enzyme inducible nitric oxide synthase (iNOS), which may be associated to its anti-inflammatory activity.

The biological properties of *A. oleracea* have been studied due to its widespread use in traditional medicine. For instance, Jambu leaves are known to contain a wide range of phenolic compounds, including vanillic acid, chlorogenic acid, scopoletin, and trans-ferulic acid, as well as flavonoids and tannins, reported to feature antioxidant and anti-inflammatory activities. Furthermore, such bioactive molecules may be involved in the biological properties of the species (Abdul-Rahim et al., 2021). Moreover, several terpenes have also been identified that may play a direct role in the anti-inflammatory, anti-tumor, and bactericidal effects of Jambu (Lalthanpuii et al., 2018; Murthy and Kee-Yeoup, 2021; Savic et al., 2021).

However, the effect of *A. oleracea* against the major microorganisms causing wound infection, its ability to promote cell migration, and a more comprehensive investigation of its antioxidant and anti-inflammatory activities remain unexplored. Thus, the aim of this work is to characterize the phytocomponents of methanol extracts of *A. oleracea leaves* by UFLC-TOF-MS and to explore the antioxidant, anti-inflammatory, antimicrobial, and healing potential focusing on its application for wounds management.

2. Material and methods

2.1. Plant material

A. oleracea leaves were obtained at the Federal Institute of Education Science and Technology of Mato Grosso (IFMT) in Sorriso - Brazil, coordinates 12°41′39.98″ S; 55°48′22.04″ W, in May 2019. The species was identified as *Acmella oleracea* (L.) R. K. Jansen (SISGEN/Brazil A114768) and the plant name was confirmed on the website www.theplantlist.org on May 6, 2024. Voucher specimens (DRG 786) of leaves of *A. oleracea* have been deposited in the herbarium of the IFMT.

2.2. Extract preparation

The leaves of *A. oleracea* were dried at 50 °C in a forced-air oven (Tecnal, TE-394/3 MP, Brasil) and crushed in an electric mill (Marconi®, MA048), yielding 898.61 g of dry plant material. The static maceration was carried out at room temperature using methanol as the liquid phase until extraction of the plant material was complete (40 days). The excess solvent was evaporated at reduced pressure in a rotary evaporator (Buchi Labortechnik AG V-700) and the methanolic extract of *A. oleracea* leaves (AOM) was obtained.

2.3. Total phenolic content

The total phenolic content was estimated according to Folin and Ciocalteu (1927), with modifications. A stock solution of AOM at 1 mg/mL was prepared in methanol (MeOH). A standard curve was plotted using tannic acid as standard. The absorbance was read at 770 nm in a UV–Vis spectrophotometer (Thermo Scientific Multiskan GO, software 3.2). The total phenolic content (TPC) was reported in μg/mg of plant extract in tannic acid equivalent (TAE). The assay was carried out in triplicate.

2.4. UFLC-QTOF-MS analysis

AOM was analyzed by ultra-fast liquid chromatography combined with mass spectrometry using a Shimadzu UFLC (Nexera model) and a Bruker mass spectrometer (QTOF Compact model) with an electrospray ionization device on positive ion mode. A Kinetex 2.6 μm, C18-100A, 100 mm × 3.0 mm column was used. Phase A of the mobile phase was water acidified with formic acid at pH = 3, phase B was methanol, the flow rate was 0.4 mL/min for a 20-min run time. Phase B initially comprised 40% of the chromatographic run, increasing to 70% at 12.20 min and 95% at 15.70 min. Then, the mobile phase was switched back to 40% B at 17.20 min to rebalance the column, until 18.50 min and the run was finished at 20 min. The electrospray voltage of the ion source was set to 40 V, the capillary voltage was set to 4500 V, and the capillary temperature was set to 220 °C. The entire mass scan was performed by scanning in the range of 100–1000 m/z. The results were compared with reports and reference standards for *A. oleracea* and related species.

2.5. Cell viability

2.5.1. Cell culture conditions

L929 fibroblasts (ATCC®CCL-1 NCTC) were cultured in Dulbecco's modified Eagle's medium (DMEM), 10% fetal bovine serum (FBS) and 1% antibiotics streptomycin and penicillin. BALB/c peritoneal macrophages were cultured in RPMI-1640 medium plus 2Mn L-glutamine, 1% antibiotics streptomycin, 5% SFB, and penicillin. Both cell lines were maintained in a humidified oven at 37 °C and 5% CO_2. Male BALB/c mice, weighing 20–25 g at 30 days of age, were obtained from the Reproductive Biology Centre of the Federal University of Juiz de Fora. The procedure was accepted by the Committee on the Ethics of Animal Experiments of the Federal University of Juiz de Fora on May 10, 2018 (Protocol Number: 07/2018-CEUA).

2.5.2. MTT reduction test

The macrophages at 2×10^5 cells/well and the fibroblasts at 5×10^3 cells/well were added to 96-well microplates and exposed to AOM diluted in 0.06% dimethyl sulfoxide (DMSO) at concentrations ranging from 18.75 to 300.00 μg/mL. DMSO 0.06% was used as a negative control. After 48h of incubation, the cytotoxicity was evaluated by cell viability using the 3-(4,5-dimethyl-2-thiazolyl)-2,5-diphenyl-2*H*-tetrazolium bromide (MTT) test (Mosmann, 1983). Absorbance was measured at 570 nm using a UV–Vis spectrophotometer (Thermo-Scientific Skanlt® Multiskan GO, software 3.2). The assay was performed in triplicate and data were presented as a percentage of cell viability.

2.6. Antioxidant activity

2.6.1. Evaluation of ROS production

ROS levels were evaluated in macrophages using 2′,7′-dichlorodihydrofluorescein diacetate (H2DCFDA) (Stroppa et al., 2017). Cells were cultured and incubated as previously described in section 2.5.1. The macrophages were treated with AOM diluted in 0.06% DMSO at concentrations ranging from 18.75 to 300.00 μg/mL and stimulated with LPS at 1 μg/mL and IFN-γ at 1 ng/mL. Unstimulated cells and stimulated cells treated with DMSO (vehicle) were used as basal and control groups, respectively. After 48h, the cells were washed in phosphate buffered saline (PBS) and incubated with H2DCFDA (1 mM) for 30 min in dark. ROS production was assessed by fluorescence (FLx800, BioTek Instruments, Inc., Winooski, VT, USA) in the culture supernatants at 485/528 nm excitation and emission, respectively. The results are expressed as the mean ± standard deviation of the fluorescence intensity (A.U) and the inhibitory concentration of 50% (IC_{50}) in μg/mL. Experiments were performed in triplicate.

2.6.2. NO scavenging assay

Nitric oxide (NO) scavenging activity was evaluated by the Griess reaction according to Jin et al. (2015), with modifications. Stock solutions of AOM and the positive control (gallic acid) were prepared in 0.1 M PBS (pH 7.4) and successively diluted to concentrations between 7.81 and 250.00 μg/mL. The samples were diluted in 10 mM sodium nitroprusside (SNP) solution, added to a 96-well microplate and incubated for 1 h at room temperature in the presence of light. As a negative control, AOM was replaced with an equivalent amount of 0.1 M PBS. After the incubation, 125 μL of Griess reagent (1% sulfanilamide and 0.1% N-(1-naphthyl)-ethylene diamine hydrochloride in 2,5% phosphoric acid) were added to each well. After 10 min incubation in dark environment, the absorbance was measured at 540 nm in a UV–Vis spectrophotometer (Thermo Scientific Multiskan GO, software 3.2). The results were expressed as mean ± standard deviation of the percentage of NO radical inhibition and the inhibitory concentration of 50% (IC_{50})

in μg/mL. The experiment was performed in triplicate.

2.6.3. DPPH scavenging activity

2,2-diphenyl-1-picrylhydrazyl (DPPH) scavenging activity was evaluated according to Brand-Williams et al. (1995), with modifications. Stock solutions of AOM and positive controls (quercetin and rutin) at 1 mg/mL in MeOH were successively diluted to provide concentrations between 0.49 and 250.00 μg/mL. The samples and DPPH solution at 20 μg/mL in MeOH were then added to a 96-well microplate. After incubation for 30 min in the dark, the absorbance was read at 517 nm in a UV–Vis spectrophotometer (Thermo Scientific Multiskan GO, software 3.2). The results are expressed as the mean ± standard deviation of IC_{50} (50% inhibitory concentration), in μg/mL. The experiment was performed in triplicate.

2.6.4. Total antioxidant capacity

Total antioxidant capacity was determined by the phosphomolybdenum complex reduction assay according to Prieto et al. (1999). A hydroalcoholic solution (MeOH: H_2O, 1:1) was used to dissolve AOM and the positive controls, quercetin and rutin, to a final concentration of 0.5 mg/mL. The absorbance of each sample was measured at 695 nm on a UV–Vis spectrophotometer (ThermoScientific Skanlt® Multiskan GO, software 3.2). The assay was carried out in triplicate. Data were expressed as mean ± standard deviation of the percentage of relative antioxidant activity (RAA%) for quercetin and rutin as follows:

$$RAA\% = \frac{Abs(AOM) - Abs(AOMblank)}{Abs(control) - Abs(controlblank)}$$

Where Abs (AOM) means the absorbance of the extract; Abs (AOM blank) means the absorbance of the blank of the extract; Abs (control) is the absorbance of the positive controls (quercetin and rutin); and Abs (control blank) is the absorbance of the blank of the positive controls.

2.6.5. Inhibition of lipid preoccupation

Inhibition of lipid peroxidation was estimated by the malondialdehyde (MDA) assay according to Osawa et al. (2005), with modifications. AOM and positive control (rutin) were dissolved in methanol at 7.50, 15.00, and 20.00 mg/mL. After being placed in sealed amber bottles, the samples, ground meat, and distilled water were kept at 5 °C for a period of seven days. 0.50 g of each sample, 1.25 mL thiobarbituric acid (TBA), 2.5 mL phosphoric acid at 1%, and 50 μL butylated hydroxytoluene (BHT) were transferred to test tubes. The absorbance of the supernatant containing the MDA-TBA complex was then measured at 535 nm in a UV–Vis spectrophotometer (ThermoScientific Skanlt® Multiskan GO, software 3.2). This procedure was performed on days 0, 2, 4, 6 and 8. A standard curve was plotted using MDA standard. The assay was carried out in triplicate.

2.7. Anti-inflammatory activity

2.7.1. NO production

NO production was assessed by indirect NO measurement using nitrite dosing according to the Griess method as described by Sun et al. (2003). Peritoneal macrophages were treated with AOM diluted in 0.06% DMSO at concentrations between 18.75 and 300.00 μg/mL and incubated for 1h. Cells were then stimulated with IFN-γ at 1 ng/mL and LPS at 1 μg/mL, and incubated for 48 h as previously described in section 2.5.1. The supernatants and Griess reagent were added to a 96-well microplate and incubated at room temperature for 10 min. The absorbance was then measured at 540 nm using a UV–Vis spectrophotometer (ThermoScientific Skanlt® Multiskan GO, software 3.2). Unstimulated cells and stimulated cells treated with DMSO (vehicle) were used as basal and control groups, respectively. A standard curve was plotted using a standard of sodium nitrite ($NaNO_2$). The results are expressed as the mean ± standard deviation of IC_{50} (50% inhibitory concentration), in μg/mL. The experiment was performed in triplicate.

2.7.2. Accumulation of lipid droplets (LDs)

The accumulation of LDs was determined according to Basselin and Robert-Gero (1998), with modifications. Peritoneal macrophages were treated with AOM diluted in 0.06% DMSO at concentrations of 150.00 and 300.00 μg/mL. After 1 h of incubation, the cells were stimulated with LPS at 1 μg/mL and IFN-γ at 1 ng/mL and incubated for 48 h, as described in section 2.5.1. After washing in PBS, the cells were stained with 200 μL Nile Red (10 μg/mL) at 25 °C for 20 min. Measurements were performed in triplicate using a spectrofluorometer (FLx800, Bio-Tek Instruments, Inc., Winooski, VT, USA), at 485 nm (excitation) and 528 nm (emission). The results are expressed as the mean ± standard deviation of the fluorescence intensity (A.U).

2.7.3. TNF-α and IL-6 production

The pro-inflammatory cytokines TNF-α and IL-6 production were evaluated in the culture supernatant by sandwich Enzyme-Linked Immunosorbent Assay (ELISA). Peritoneal macrophages were treated with AOM diluted in 0.06% DMSO at concentrations of 150.00 and 300.00 μg/mL, and incubated for 6 h. Then, the cells were stimulated with LPS at 1 μg/mL and IFN-γ at 1 ng/mL, and incubated for 24 h, as described in section 2.5.1. Cytokine concentrations were determined in the culture supernatant using a commercially available BD OptEIATM kit (BD Biosciences), according to the manufacturer's instructions. The absorbances were measured at 450 nm in a UV–Vis spectrophotometer (ThermoScientific Skanlt® Multiskan GO, software 3.2). Cytokine concentrations are expressed in pg/mL and were determined using a standard curve. The experiment was performed in triplicate.

2.8. Antibacterial and antifungal activity

2.8.1. Bacterial and fungal strains

The following strains were used to analyze the antibacterial activity of the extract: *Escherichia coli* (ATCC® 10536™), *Staphylococcus epidermidis* (ATCC® 0016™), methicillin-resistant *Staphylococcus aureus* (ATCC® 33591™) and *Pseudomonas aeruginosa* (INCAS 2742). The bacterial strains were cultured for 24 h at 37 °C in Mueller Hinton (MH) culture media before each experiment. Antifungal studies were conducted using *Candida albicans* (ATCC® 10231™), resistant to fluconazole, anidulafungin, itraconazole, and voriconazole, and *C. albicans* (ATCC® 24433™), sensitive to conventional antifungal therapy. The fungal strains were cultured for 24h at 35 °C in Sabouraud (SB) culture media before each experiment.

2.8.2. Minimum inhibitory concentration (MIC)

The MIC was estimated according to the protocol defined by CLSI (CLSI modified, 2018). The bacterial and fungal strains were grown for 24h as previously described in section 2.7.2. A stock solution at 2.50 mg/mL of AOM was prepared in 10% DMSO and successively diluted to concentrations between 1000.00 and 7.80 μg/mL in a 96-well microplate. Then, 20 μL of *inoculum* was added based on the standard 0.5 McFarland scale (10^8 CFU/mL), for bacteria, and 1.0 (10^6 CFU/mL), for fungi. The microplates were incubated at 35 °C (fungi) and 37 °C (bacteria) for 24 h. The growth control (growth broth + extract + *inoculum*) and the blank (growth broth + extract) were also performed. Nystatin (10.00–0.08 μg/mL), for fungi, and azithromycin (400.00–3.12 μg/mL), for bacteria, were used as positive controls. The MIC was calculated by the lowest dilution showing complete inhibition of the strain tested. The experiment was performed in triplicate.

2.8.3. Minimum bactericidal (MBC) and fungicidal concentration (MFC)

Aliquots of 10 μL were taken from wells with no visible growth and plated on SD agar plates for fungi and MH agar plates for bacteria. Plates were incubated at 35 °C (fungi) and 37 °C (bacteria) for 24 h. The MBC and MFC are expressed as the lowest concentration of the extract that is sufficient to cause the death of the bacteria or fungi (Lemos et al., 2020). The experiment was performed in triplicate.

2.8.4. Bacterial killing assay

The effect of AOM on the growth curve for *S. aureus* and *P. aeruginosa* was performed according to Lemos et al. (2020), with modifications. Briefly, AOM at 2MIC, MIC, and 1/2 MIC concentrations, MH growth broth, and the *inoculum* based on the standard 0.5 McFarland scale (10^8 CFU/mL) were added to a 96-well microplate. The microplates were incubated at 37 °C and the absorbance was read at 595 nm at 0, 1, 2, 4, 6, 8, 12, 24, 48, and 72 h. Graphs of absorbance versus incubation time were plotted in order to evaluate evidence of bactericidal activity of AOM. Azithromycin (MIC values) was selected as the positive control. Bacterial strains inoculated in MH growth broth were used as the growth control. The experiment was performed in triplicate.

2.8.5. Evaluation of AOM on biofilms adhesion

The biofilm adhesion assay for *S. aureus* and *P. aeruginosa* was performed according to Sadan et al. (2020), with modifications. Briefly, azithromycin (positive control) or AOM (2MIC, MIC, and ½ MIC values) were incubated with *S. aureus, P. aeruginosa,* and mixed cell suspensions (10^8 CFU/mL) in 96-well microplates for 24 h at 37 °C. Mixed cell suspensions were treated with AOM at *S. aureus* 2MIC, MIC, and ½ MIC values or azithromycin at *S. aureus* MIC value. Free-floating bacterial cells were gently washed with 200 μL of saline solution. The adherent cells were then vigorously resuspended for 5 min, and the samples were analyzed by spectrophotometry at 595 nm. Experiments were performed in triplicate. Biofilm inhibition (%) was calculated using the following equation:

$$Biofilmeinhibition(\%) = \frac{ODcontrol - ODtreatment}{ODcontrol} x100$$

Where, ODtreatment: optical density of the treatment sample; ODcontrol: optical density of the growth control.

2.9. Scratch wound healing assay

The effect of AOM on the migration of L929 fibroblasts was determined according to Pereira et al. (2018) with modifications. Briefly, the cells (5×10^4 cells/well) were seeded into 24-well microplates and allowed to adhere for 24 h. Then, a linear scratch was made in the adherent cell layer using a sterile 200 μL pipette tip. The scratched area was then exposed to AOM diluted in 0.06% DMSO at concentrations of 18.75 and 37.50 μg/mL. Control samples were treated with fresh DMEM only. Images were taken at 10x magnification using a microscope (FLx800, BioTek Instruments, Inc., Winooski, VT, USA) at 0, 24, and 48 h. To assess the cell migration, the images were analyzed using the ImageJ software (version 1.54) by monitoring the scratch area at each time interval. The experiment was performed in triplicate and the cell migration rate was calculated as follows:

$$Migrationrate(\%) = \frac{Scratcharea(t0) - Scratcharea(tf)}{Scratcharea(t0)} x100$$

Where, scratch area (t0): scratch area at time 0 h; scratch area (tf): scratch area at 24, or 48 h.

2.10. Statistical analysis

ANOVA followed by Bonferroni test ($P < 0.05$) was used for statistical analysis with GraphPrism 8.0.1 software. Results presented as mean ± SD.

3. Results and discussion

3.1. Total phenolic content

Phenolic compounds are well known for their antimicrobial, antioxidant, and anti-inflammatory activities. Such phytochemicals are able to scavenge free radicals resulting from oxidative stress thereby, reducing cellular damage and contributing to the healing process (Abdul-Rahim et al., 2021). Besides, phenolic species can also affect the bacterial cell envelope, affecting ion transport, microbial adhesion, enzymatic activity, and enterotoxin production (Suriyaprom et al., 2022).

The total phenolic content of AOM was 172.88 ± 15.45 μg/mg in TAE, representing approximately 17% of the total extract composition. According to Abeysiri et al. (2013), the total phenolic content in methanolic extracts of *A. oleracea* is significantly higher in leaves (7.59 mg/g TAE) compared to flowers (5.34 mg/g TAE) and roots (2.65 mg/g TAE) ($P < 0.05$).

Nabi and Shrivastava (2016) confirmed the presence of phenolic compounds in the ethanolic extract of *A. oleracea* leaves, achieving a total phenolic content of 84.52 mg/g in TAE. Later, Nipate and Tiwari (2020) also found significant phenolic content in the ethanolic and aqueous extracts of *A. oleracea* flowers (186.21 and 121.92 μg/mL in gallic acid equivalents, respectively). These reports suggest that the total phenolic content of *A. oleracea* extracts can be variable, although our results shows that AOM had higher total phenol content compared to previous results reported in the literature.

3.2. Phytochemical identification UFLC-QTOF-MS

All the 9 compounds identified in the UFLC-QTOF analyses are described in Table 1. The peaks obtained from the identified compounds are labeled numerically according to their retention times. Compounds 2 and 4 to 9 correspond to seven N-alkylamides. These, include spilanthol [8] and its oxidation products, i.e, 8,9-dihydroxy-deca-2,6-dienoic acid isobutyl-amide [2] and 6,9-dihydroxy-deca-2,7-dienoic acid isobutyl-amide [4]. The presence of other 4 alkylamides was also identified: N-isobutyl-2,4-undecadiene-8,10-diynamide [5], N-phenethyl-2-nonene-6,8- diynamide [6], N-(2-methylbutyl)-2- undecene-8,10-diynamide [7] and N-(2-methylbutyl)- 2,6,8-decatrienamide [9]. These data are consistent with the literature, as *A. oleracea* leaves are known to be rich in this group of phytoconstituents (Lalthanpuii et al., 2018; Savic et al., 2021; Uthpala and Navaratne, 2021).

Alkylamides are secondary metabolites produced of the bonding of fatty acids, usually unsaturated, to an amine group derived from a decarboxylated amino acid. Alkylamides have been associated with diverse biological properties, including antinociceptive, anti-inflammatory and antimicrobial activity (Sharma and Arumugam, 2021). Spilanthol is the most important representative of the alkylamide class. It is an aliphatic alkylamide, responsible for most of the biological properties of *A. oleracea* (Lalthanpuii et al., 2018; Savic et al., 2021).

Vanillic acid [1] and quercetin [3] are phenolic compounds with promising antioxidant activity that has also been identified in AOM. Nevertheless, literature suggests that Jambu may be rich in other phenolic compounds such as trans-ferulic acid and scopoletin (Lalthanpuii et al., 2018; Uthpala and Navaratne, 2021). Besides, worth-noting the significant high levels of phenolic compounds in AOM found in the total phenolic content assay, which also suggest the presence of other phytoconstituents from phenolic compounds class.

3.3. Cell viability

Both macrophages and fibroblasts cells were chosen for this assay due to their involvement in all stages of wound healing and skin repair processes (Cañedo-Dorantes and Cañedo-Ayala, 2019). The MTT reduction assay was used to assess the viability of L929 fibroblasts and

Table 1
Compounds identified in the methanolic extract of leaves from *Acmella oleracea* (AOM) by UFLC-QTOF-MS.

Nº	Rt (min)	Exact mass	$[M+H]^+$ (m/z)	Fragmentation of molecular ions MS^2 (m/z)	Compound name and molecular structure	References
1	1.4	168.06166	169.0695	353.087 (2M + NH3) 191.0514 (M + Na)	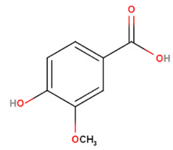 Vanillic acid	Abdul-Rahim et al. (2021)
2	2.7	277.16296	278.1708	278,1708 (M + H)	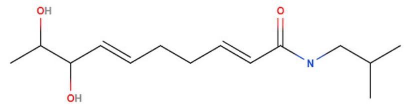 8,9-dihydroxy-deca-2,6-dienoic acid isobutyl-amide	Savic et al., 2021
3	2.8	302.0426	305.0708	305.0708 (M+3H)	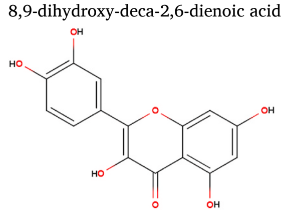 Quercetin	Nascimento et al. (2020); Kim et al. (2018)
4	2.9	277.16276	278.1706	278,1706 (M + H)	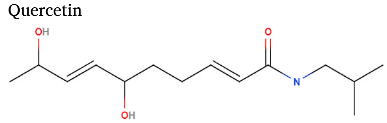 6,9-dihydroxy-deca-2,7-dienoic acid isobutyl-amide	Savic et al., 2021
5	6.5	229.14376	230.1516	481,2798 (2M + Na) 252,1335 (M + Na)	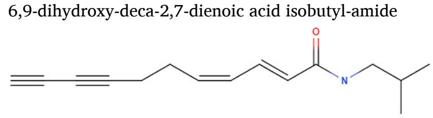 N-isobutyl-2,4- undecadiene-8,10-diynamide	Savic et al., 2021
6	6.7	251.12796	252.1358	525, 2486 (2M + Na) 274,1177 (M + Na)	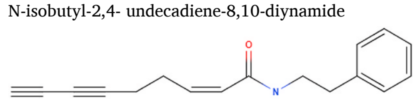 N-phenethyl-2-nonene-6,8- diynamide	Savic et al., 2021
7	7.6	246.46106	247.4689	762,3728 (3M + Na) 509,3110 (2M + NH3)	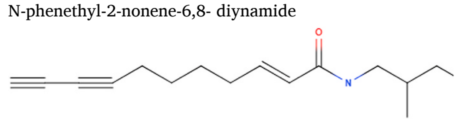 N-(2-methylbutyl)-2- undecene-8,10-diynamide	Savic et al., 2021
8	7.9	221.17606	222.1839	465,3424 (2M + Na) 222,1839 (M + H)	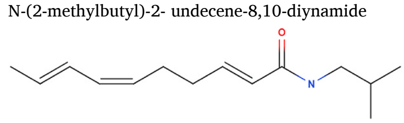 N-isobutyl-2,6,8- decatrienamide (spilanthol)	Savic et al., 2021
9	9.0	234.18366	235.1915	493,3729 (2M + Na) 236,1993 (M + H)	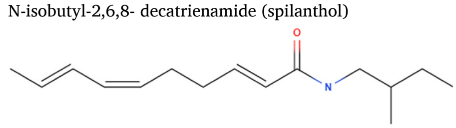 N-(2-methylbutyl)- 2,6,8-decatrienamide	Savic et al., 2021

Retention time (Rt) in minutes.

peritoneal macrophages when exposed to AOM. Only metabolically active cells may reduce MTT to formazan, the production of formazan is directly proportional to the number of viable cells in the culture (Mosmann, 1983).

According to ISO 10993–5:2009 (2009), cell viability should not be reduced below 70%, for some substance to be considered biocompatible. As shown in Fig. 1, cell viability was maintained above 70% for all concentrations of AOM tested., meaning that it did not show cytotoxicity to skin cell lines. However, a more pronounced reduction in cell viability of L929 fibroblasts was observed when exposed to AOM at 300 μg/mL. Similar results were found by Da Silva et al. (2016), which reported the cytotoxicity of the ethanolic extract of *A. oleracea* seeds at concentrations ranging from 250.00 to 1000 μg/mL. The authors also observed a significant decrease in the viability of L929 fibroblasts after 48 h of incubation at all concentrations tested. Such cell strains are reported to exhibit higher sensitivity, which allows a more accurate assessment of the cytotoxicity of the extract (Thonemann et al., 2002).

3.4. *Antioxidant activity*

The production of both reactive oxygen and nitrogen species must be considered in the whole wound healing process. Their excessive and prolonged production trigger severe cellular damage, impairing proper tissue repair. The overproduction of ROS mediates the transcription of pro-inflammatory cytokines such as IL-6, and TNF-α. It may also damage proteins from extracellular matrix (ECM) and reduce fibroblast and keratinocyte homeostatic function. Furthermore, oxidative stress and free radical production activate pro-apoptotic proteins, leading to cell

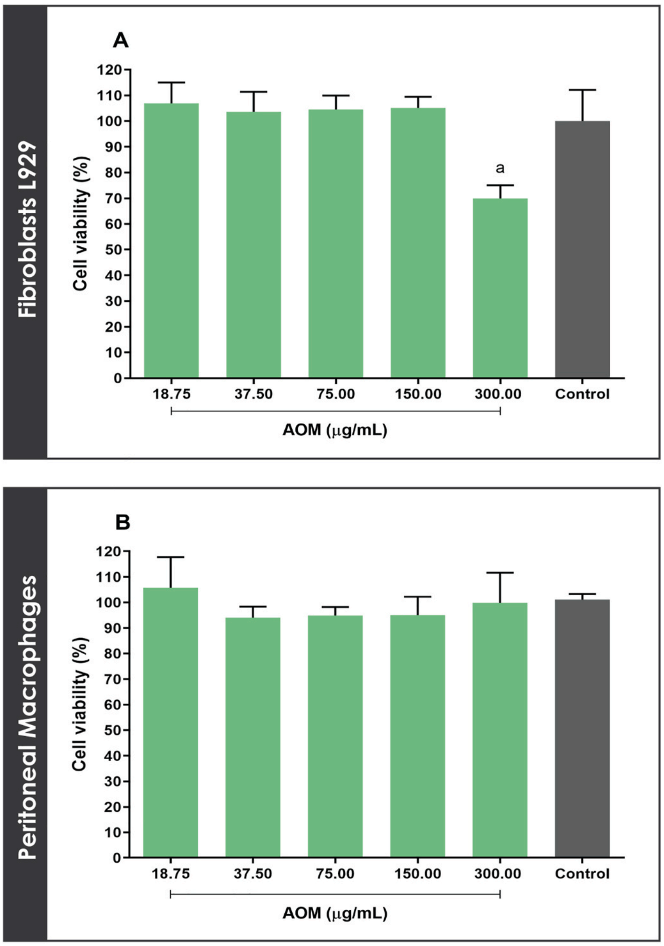

Fig. 1. Evaluation of the cell viability in the L929 fibroblasts (A) and peritoneal macrophages (B) cell lines after treatment with the methanolic extract from *A. oleracea* leaves (AOM). Control - cells cultured in a medium added to vehicle (DMSO). a - Statistical difference from Control ($P < 0.05$). ANOVA followed by the Bonferroni test.

death. Therefore, compounds that modulate the excessive production of ROS, NO and other free radicals may play an essential role in the wound healing process (Chin et al., 2019; Dunnill et al., 2017; Larouche et al., 2018).

The influence of AOM treatment on macrophage ROS production was evaluated fluorometrically. The results, expressed as fluorescence intensity (A.U), showed that AOM significantly reduced ($p < 0.05$) ROS production for all the concentrations evaluated (Fig. 2A). The extract exhibited an IC_{50} value of 25.06 ± 4.84 μg/mL. In addition, at the highest concentration (300.00 μg/mL), AOM showed a reduction in ROS production of approximately 69.03 ± 3.85%, which was not statistically different from the basal control ($p < 0.05$).

Gay et al. (2018) investigated the effects of vanillic acid and trans-ferulic acid, both found in *A. oleracea* species. After 24 h, the authors reported that these compounds reduced intracellular ROS production in neuronal cells and attenuated oxidative stress-mediated cell death. These findings suggest a relationship between the high levels of total phenolics found in this study and the antioxidant activity of AOM, which, in this case produced a neuroprotective effect.

NO is a chemical mediator with multiple biological functions, such as antimicrobial, vascular homeostasis, neurotransmission, and antitumor activities. Furthermore, NO can react with superoxide anion (O_2^-) to generate peroxynitrite ($ONOO^-$), a potent oxidant agent. Therefore, the NO scavenging assay was carried out to assess the ability of AOM to prevent the formation of nitrite ions *in vitro*. Such method is based on the fact that NPS spontaneously generates NO in aqueous solution in physiological pH, which reacts with oxygen to yield nitrite ions, quantified by the Griess test. (Patel and Patel, 2011).

Fig. 2B shows that AOM inhibited the production of nitrite ions in a dose-dependent manner. In fact, AOM at 250 μg/ml reduced aproximatel 73.47 ± 1.95% of nitrite production ($p < 0.05$), which might due to a considerable antioxidant activity, reducing the dose needed to produce 50% of inhibitory result (i.e., IC_{50}). AOM showed IC_{50} of 127.6 ± 14.42 μg/mL, a value statistically smaller than the positive control (227.95 ± 3.46 μg/mL) ($p < 0.05$). The results reported by Lalthanpuii et al. (2017), showed that the aqueous extract of the aerial parts of *A. oleracea* produced a dose-dependent nitrite inhibition, with IC_{50} of approximately 80 μg/mL, a value significantly lower than the one we found for AOM. It is possible that AOM, object of our work, had higher content of antioxidant compounds, which would be responsible for such result.

The DPPH radical scavenging assay was used to evaluate the ability of AOM compounds to donate hydrogen atoms (Santos-sanchéz et al., 2019). AOM exhibited an IC_{50} value of 44.50 ± 4.46 μg/mL (Table 2), which was statistically superior than the positive controls: Rutin (0.44 ± 0.22 μg/mL) and Quercetin (0.37 ± 0.02 μg/mL) ($p < 0.05$). Thakur et al. (2019) also evaluated the antioxidant activity of Jambu extracts using the DPPH radical scavenging assay and concluded that the methanol extracts of roots, leaves and flowers IC_{50} values ranging from 67.34 to 127.19 μg/mL. It is important to note that a wide range of methodological and environmental factors can affect the antioxidant activity of a general plant extract. These include the type of solvent used for extraction, the season in which the plant was collected, the stage of its development and age, the part of the plant used, and the soil conditions (Thakur et al., 2019).

The total antioxidant capacity of AOM was also investigated by the phosphomolybdenum complex reduction assay, as this test demonstrates the antioxidant activity of compounds whether soluble or insoluble in aqueous medium. (Prieto et al., 1999). The RRA% of rutin and quercetin for the AOM were 104.01 ± 21.29% and 63.56 ± 13.01%, respectively (Table 2). These results suggest that the antioxidant power of the compounds present in AOM is similar to that of rutin and corroborate our findings and the widely known antioxidant potential of AOM. Indeed, AOM content is greatly componed alkylamides. Nevertheless, alkylamides shows free radical rapid scavenging activity, which is known to last for one week (Dallazen et al., 2020). Therefore, the high phenolic content of the extract should be closely related to the significant total antioxidant potential of AOM. It is noteworthy that no previous reports were found on the total antioxidant capacity of *A. oleracea*, species of the same genus, or yet for spilanthol alone.

Aldehydes are produced as consequence of lipid peroxidation induced by excessive production of free radicals, being considered highly toxic to cells homeostatic metabolism (Yadav and Ramana, 2013). The inhibition assay uses MDA as a biomarker of lipid peroxidation therefore, it's expected that antioxidant samples should inhibit MDA production (Elbadrawy and Sello, 2016). The results showed that AOM was able to significantly inhibit MDA production from the day 2, being statistically different from the negative control (Fig. 2C). At the end of day 8, 30 μg/mL of AOM showed an inhibition of about 63,69 ± 3.47%. AOM at 15.00 and 7.50 μg/mL inhibited MDA production by approximately 46.55 ± 3.28% and 40.80 ± 7.90%, respectively. These results were equivalent to those found for the same concentrations of BHT (positive control) ($p < 0.05$).

No studies were found on the inhibition of lipid peroxidation by *A. oleracea*. However, Gonçalves et al. (2021) evaluated the inhibition of oxidative stress in the brains of mice treated orally with the ethanolic extract of *Acmella ciliata,* which belongs to the same genus as *A. oleracea* and is also known for its high alkylamides content. The extract significantly reduced MDA production and increased levels of antioxidant markers in mice ($p < 0.0001$).

The results discussed above highlight the antioxidant potential of

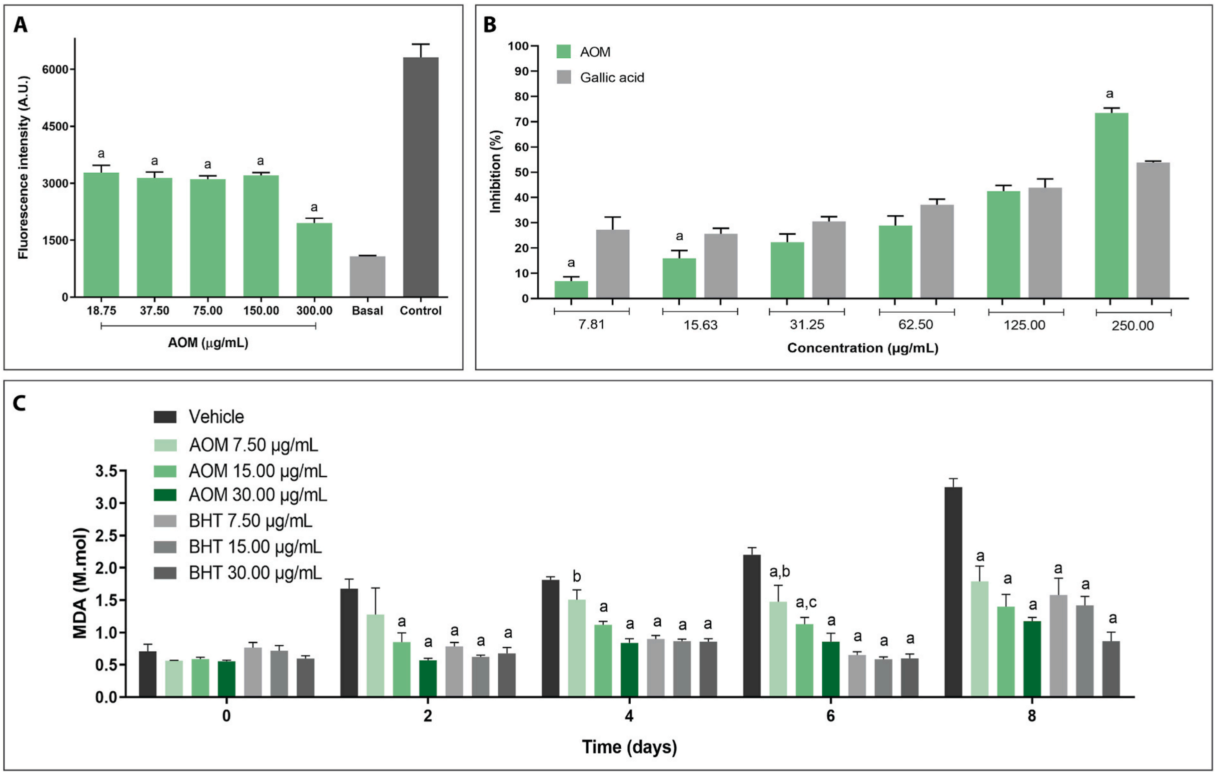

Fig. 2. Antioxidant activity of the methanolic extract from *A. oleracea* leaves (AOM). (A) Reduction of reactive oxygen species (ROS) levels in macrophages after treatment with the AOM. Basal - Unstimulated cells treated with DMSO (vehicle). Control – Stimulated cells (INF-γ + LPS) treated with DMSO (vehicle). a - Statistical difference from control ($P < 0.05$). (B) Nitric oxide scavenging activity of the AOM. Galic acid was employed as positive control. a - Statistical difference from galic acid ($P < 0.05$). (C) Inhibition of malondialdehyde formation in the presence of the AOM. Butylhydroxytoluene (BHT) was employed as positive control. a - Statistical difference from vehicle ($P < 0.05$). b - Statistical difference between AOM 7.5 and BHT 7.5 μg/mL concentrations ($P < 0.05$). c - Statistical difference between AOM 15.00 and BHT 15.00 μg/mL concentrations ($P < 0.05$). ANOVA followed by the Bonferroni test.

Table 2
Evaluation of antioxidant activity of methanolic extract from *Acmella oleracea* leaves (AOM) by DPPH and phosphomolybdenum assays.

Samples	DPPH• – IC_{50} (μg/mL)	Phosphomolybdenum	
		% relative of rutin	% relative of quercetin
AOM	44.50 ± 4.46 [a,b]	104.01 ± 21.29	63.56 ± 13.01
Rutin	0.44 ± 0.22	–	–
Quercetin	0.37 ± 0.02	–	–

ANOVA followed by the Bonferroni test.
[a] Statistical difference from positive control rutin ($P < 0.05$).
[b] Statistical difference from positive control quercetin ($P < 0.05$).

A. oleracea extract through a wide range of oxidative pathways and support, in a very robust way, AOM as an important natural source of antioxidants. Therefore, AOM may help prevent the progression of oxidative stress-related and redox-imbalanced disorders, including difficult-to-heal and chronic wounds. Nascimento et al. (2020) studied the antioxidant capacity of ethanol extracts from different parts of *A. oleracea*. Their results showed greater antioxidant capacity for leaves extracts, which correlates directly with the higher content of phenolic compounds and flavonoids.

It is important to highlight that extracts prepared with more polar solvents feature greater free radical scavenging activity than those prepared with non-polar solvents. This may be related to the higher extraction of polyphenols by polar solvents, including methanol, ethanol and water (Dallazen et al., 2020). Besides, although alkylamides may not be the main antioxidant compounds in AOM, their synergistic effect should also be considered, since the antioxidant capacity of alkylamides is not associated with scavenging free radicals, but with preventing the migration of inflammatory cells, respiratory burst and ROS production. (Dallazen et al., 2020; Nascimento et al., 2020; Silva et al., 2023).

3.5. Anti-inflammatory activity

NO production can be closely related to the inflammatory stage of wound healing, as it is produced by leukocytes. However, the massive NO production can be harmful to surrounding tissues, leading to an excessive or chronic inflammatory response (Bernatchez et al., 2013; Man et al., 2022). Cellular NO production was measured by the Griess test in the supernatant of peritoneal macrophage cultures treated with AOM at the same concentrations used in the MTT cell viability assay.

AOM significantly ($p < 0.05$) reduced NO levels at all concentrations tested, except for 18.75 μg/mL concentration (Fig. 3C). AOM inhibited approximately 99.21 ± 3.82% and 81.20 ± 8.25% of NO production at 300.00 and 150.00 μg/mL, respectively, and showed an IC_{50} value of 74.78 ± 2.09 μg/mL. According to Stein et al. (2021), ethanolic extracts from the flowers and leaves of *A. oleracea* (25–100 μg/mL), as well as isolated spilanthol (50–200 μM), were able to significantly reduce the *in vitro* generation of NO by vascular smooth muscle cells stimulated with hyperglycemic medium ($p < 0.05$). These results suggest that AOM phytoconstituents feature ability to reduce NO synthesis, which is consistent with the antioxidant activity described by our results.

Lipid droplets (LDs) are organelles found in the cytoplasm of various cell types, including leukocytes, in which their accumulation is greater once the inflammatory process occurs. In this case, LDs are associated with the production of inflammatory mediators, such as prostaglandins and leukotrienes (Melo and Weller, 2016). Here, intracellular accumulation of LDs was assessed in peritoneal macrophages cell cultures treated with AOM at 150.00 and 300.00 μg/mL (Fig. 3A and B). The

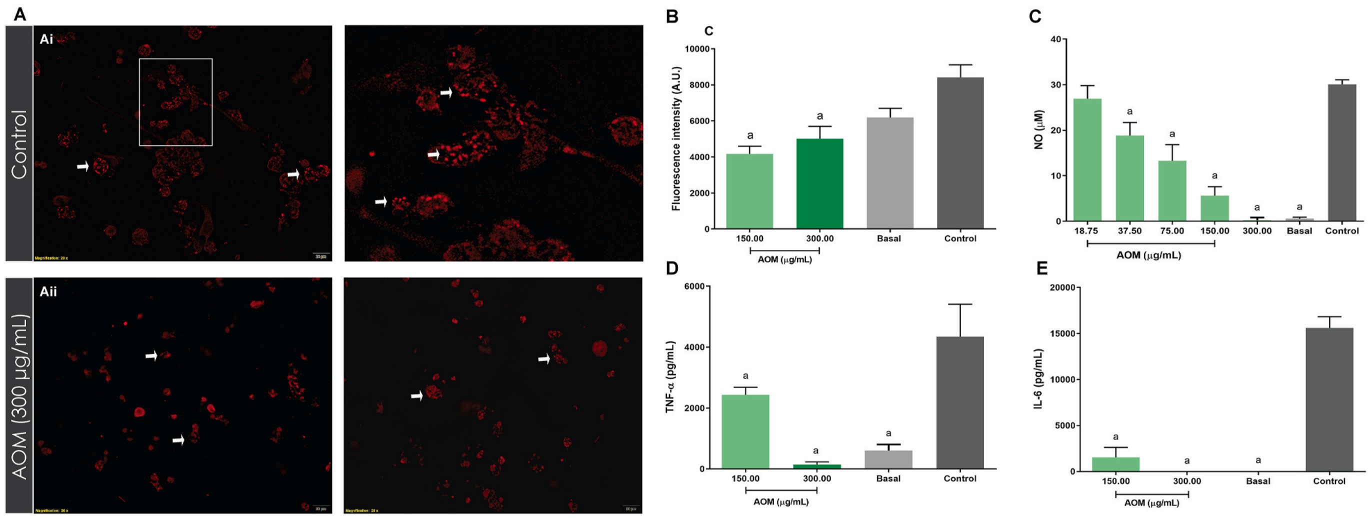

Fig. 3. Anti-inflammatory activity of the methanolic extract from *A. oleracea* leaves (AOM). (A) Cytoplasmic lipid droplets by fluorescence microscopy stained with Nile Red (10 μg/mL) in peritoneal macrophages. Ai: Stimulated cells (INF-γ + LPS) treated with DMSO (vehicle). Aii: Stimulated cells (INF-γ + LPS) treated with AOM at 300.00 μg/mL (B) Lipid droplets, (C) nitric oxide, (D) TNF-α and (E) IL-6 production by peritoneal macrophages after treatment with AOM. Basal - Unstimulated cells treated with DMSO (vehicle). Control – Stimulated cells (INF-γ + LPS) treated with DMSO (vehicle). a - Statistical difference from control ($P < 0.05$). ANOVA followed by the Bonferroni test. (For interpretation of the references to colour in this figure legend, the reader is referred to the Web version of this article.)

intracellular accumulation of LDs was dramatically reduced at AOM concentrations of 150.00 μg/mL (54.30 ± 7.94%) and 300.00 μg/mL (67.51 ± 0.72%), compared to the control ($p < 0.05$). To date, this is the first time such a reduction in intracellular LD accumulation by AOM has been reported. This potent effect could be linked to the ability of AOM phytoconstituents to inhibit the production of key inflammatory mediators like prostaglandins (Sharma and Arumugam, 2021).

TNF-α and IL-6, pro-inflammatory interleukins secreted by macrophages, neutrophils and leukocytes, linked to the chemotaxis of inflammatory cells to the wound site. Interestingly, IL-6 is also associated with increased fibroblast proliferation (Gushiken et al., 2021). Increased and prolonged production of both cytokines enhances the secretion of matrix metalloproteinases (MMP) 1 and 2, thereby favoring wound chronicity, due to excessive ECM destruction (Chin et al., 2019; Larouche et al., 2018).

Both TNF-α and IL-6 levels were assessed by ELISA of peritoneal macrophage cell cultures treated with AOM at concentrations of 150.00 and 300.00 μg/mL. At 150.00 μg/mL, AOM reduced the release of the cytokines IL-6 and TNF-α by 90.12 ± 6.86% and 41.46 ± 3.14%, respectively, while at 300 μg/mL, AOM reduced the release of IL-6 and TNF-α by 100.00% and 96.66 ± 1.95%, respectively, compared to the control ($p < 0.05$) (Fig. 3D and E). Previously published data attribute the anti-inflammatory effects of *A. oleracea* mainly to spilanthol. For instance, Blanco et al. (2018) showed that spilanthol inhibited the release of IL-8 and TNF-α by LPS-stimulated neutrophils cells ($p < 0.001$). The anti-inflammatory effect of spilanthol was also confirmed by the results reported by Huang et al. (2018). The authors found that spilanthol reduced the production of pro-inflammatory cytokines released by HaCaT cells, including TNF-α, IL-6, and IL-8. These findings suggest that a significant contribution of spilanthol and alkylamides for the anti-inflammatory effects of *A. oleracea* extracts.

Gene inhibition of inflammatory mediator genes seems to be one of the anti-inflammatory mechanisms of *A. oleracea*. According to Kim et al. (2018), the methanolic extract of *A. oleracea* was effective in inhibiting the transcription factor NF-κB in RAW 264.7 macrophages cell strain, which is required for the induction of a variety of pro-inflammatory genes. Furthermore, Bakondi et al. (2019) showed that spilanthol reduced NO production by inhibiting the expression of the inducible nitric oxide (iNOS)-related genes.

Taken together, our results help to clarify the mechanistic anti-inflammatory activity of AOM. Indeed, the anti-inflammatory activity of Jambu is mainly attributed to alkylamides and phenolic compounds such as vanillic acid, quercetin, scopoletin and trans-ferulic acid (Bakondi et al., 2019; Boonen et al., 2012). Although some studies have provided evidence for the anti-inflammatory potential of this species (Uthpala and Navaratne, 2021), the mechanisms responsible for this activity remain to be fully elucidated.

3.6. Antimicrobial activity

Wound infection has a direct effect on wound healing progress by increasing the release of pro-inflammatory mediators, triggering the development of chronic wounds, abscess formation and even sepsis. Gram-positive bacteria such as *S. aureus* and *S. epidermidis* are most commonly isolated in the early stages of a skin lesion, while gram-negative bacteria including *E. coli* and *P. aeruginosa*, and some fungi, such as *C. albicans*, are more common in chronic wounds, as they tend to colonize deeper skin layers (Simões et al., 2018; Yazarlu et al., 2021).

Azithromycin is a broad-spectrum antibiotic in the macrolide group, commonly used to treat respiratory and skin infections (Abruzzo et al., 2022), being active against Gram-positive and some gram-negative bacteria. However, the emergence of resistant strains, including methicillin-resistant *S. aureus* (MRSA), has made the treatment of skin infections more difficult (Zhou et al., 2023).

The antibacterial and antifungal activities were first evaluated by determining the MIC values (Table 3). The MIC values of AOM against *E. coli, S. epidermidis,* and methicillin-resistant *S. aureus were* were 1000 μg/mL, while AOM MIC of 500.00 μg/mL was found to *P. aeruginosa*. AOM produce bactericidal activitiy at the MIC value against *P. aeruginosa*, and showed bacteriostatic effect for *E. coli, S. epidermidis,* and *S. aureus*. Moreover, the MIC values of AOM for both *C. albicans* strains were 125.00 μg/mL, with fungistatic effect.

Uthpala et al. (2021) investigated the antimicrobial potential of aqueous and ethanolic extracts of *A. oleracea* flowers and stems. The authors found MIC values ranging from 312.5 to 1250 μg/mL against *P. aeruginosa, B. subtilis, S. aureus, E. coli,* and *C. albicans*. Moreover, our research group has previously demonstrated antifungal activity of spilanthol against a multi-resistant strain of *C. albicans*. Spilanthol was related to cell lipid membrane disruption of fungi cell membranes, being more effectively than nystatin, which was used as a positive control (Fabri et al., 2021).

According to Table 3, *S aureus* were resistant to azithromycin as their

Tables 3
In vitro antibacterial and antifungal activities of methanolic extract from *A. oleracea* leaves (AOM) for the microtiter dilution broth assay.

Microrganism	MIC with AOM (μg/mL)	Effect at MIC value	MBC or MFC (μg/mL)	MIC with azithromycin (μg/mL)	MIC with nystatin (μg/mL)
Escherichia coli (ATCC® 10536™)	1000	Bacteriostatic	>1000	6.25	–
Staphylococcus epidermidis (ATCC® 0016™)	1000	Bacteriostatic	>1000	3.12	–
Staphylococcus aureus (ATCC® 33591™)	1000	Bacteriostatic	>1000	400.0	–
Pseudomonas aeruginosa (INCAS 2742)	500	Bactericidal	500	100.0	–
Candida albicans (ATCC® 24433™)	125	Fungiostatic	500	–	2.5
Candida albicans (ATCC® 10231™)	125	Fungiostatic	500	–	2.5

MIC - Minimum inhibitory concentration; MBC - Minimum bactericidal concentration; MFC - Minimum fungicidal concentration; Azithromycin - positive control for bacterial strains; Nystatin - Positive control for fungal strains.

MIC values exceeded the CLSI MIC breakpoints (*Staphylococcus* species: ≥8 μg/mL) (CLSI, 2020). This result is expected as ATCC® 33591™ is an MRSA. The MIC value of *P. aeruginosa* also indicated antimicrobial resistance, which is explained by the poor diffusion of macrolides across the membrane of Gram-negative bacilli (Meerwein et al., 2020). These results support the search for therapeutic alternatives for skin infections and justify the use of azithromycin as a comparative control in the biofilm and growth curve assays.

P. aeruginosa and *S. aureus,* commonly isolated from chronic wounds (Chin et al., 2019), also exhibited resistance to azithromycin in the MIC assay and were, therefore, selected for the following tests. To understand antimicrobial activity over time, it is also important to monitor the bacterial growth curve under AOM treatment. Area under the curve (AUC) was significantly reduced for both *S. aureus* and *P. aeruginosa* growth for AOM and azithromycin in comparison with control group ($p < 0.05$; Fig. 4A and B). *S. aureus* treated with AOM at MIC and ½ MIC values showed 77.16 ± 1.50% and 22.38 ± 2.86% bacterial growth reduction, respectively. Similarly, *P. aeruginosa* growth was inhibited by 62.36 ± 1.01% and 56.26 ± 3.10% at MIC and ½ MIC values, respectively. Furthermore, AOM treatment (2-fold-MIC, MIC values) resulted in superior *S. aureus* growth inhibition compared to azithromycin. AOM at 2-fold-MIC and azithromycin inhibited *P. aeruginosa* growth in a similar behavior ($p < 0.05$).

In fact, compared to the growth control, AOM treatment at the MIC value prolonged the lag phase from 4h to 12h and caused a decrease in the growth cycle curve (log phase), while AOM at 2-fold-MIC concentration produced bactericidal effect for both bacteria tested (Fig. 4Ai, 4Bi). Such factors may be related to disturbances in cellular integrity and impairment in the production of cellular components required for bacterial proper growth (Fabri et al., 2021).

The activity of AOM on biofilm formation was demonstrated by a reduction in optical density compared to the growth controls (Fig. 5). The results indicated that the inhibition of biofilm formation for AOM at MIC values were 44.71% ± 4.44, 95.50% ± 6.37, and 51.83% ± 1.50 for *S. aureus, P. aeruginosa* and mixed biofilms, respectively, which were statistically similar to azithromycin, used as a positive control ($p < 0.05$). AOM at 2-fold-MIC value demonstrated superior antibiofilm activity against methicillin-resistant *S. aureus* and mixed biofilms compared to azithromycin ($p < 0.05$). MRSA biofilms pose a significant challenge to wound management due to their resistance to a variety of antibiotics and inability to be easily eradicated by the immune system (Zhou et al., 2023).

Biofilms have a protective effect on microorganisms, increasing their survival while decreasing the effectiveness of antibiotics. Biofilm formation is a major cause of chronic wound development (Clinton and Carter, 2015). According to Clinton and Carter (2015), less than 10% of acute wounds contain biofilms, while more than 60% of chronic wounds do. Therefore, alternative treatments to inhibit biofilm formation are of great importance to improve wound healing treatments.

The antibiofilm potential of Jambu has been investigated by Peretti et al. (2021), that studied the ability of a hydroethanolic extract from the leaves of *A. oleracea* to disrupt preformed *S. mutans* biofilms. *A. oleracea* extracts reduced biofilm viability by 50%, similar to the positive control ($p < 0.05$). Such results highlight the potential of AOM as a promising broad-spectrum inhibitor of bacterial and fungal growth. These findings support the traditional use of Jambu to treat respiratory and wound infections (Araújo et al., 2021; Bellumori et al., 2022; Elufioye et al., 2020). The antimicrobial activity of AOM may be related to the presence of alkylamides, such as spilanthol and the phenolic metabolite vanillin acid, identified in this study. Those bioactive molecules are capable of affecting the microbial cell membrane, causing it to rupture (Fabri et al., 2021; Peretti et al., 2021).

3.7. Wound healing activity

Fibroblast migration and proliferation are fundamental to tissue repair during the proliferative stage of wound repair, as they are involved in wound contraction, increased collagen deposition and ECM synthesis (Pitz et al., 2016; Sung et al., 2020). Therefore, compounds capable of enhancing cell migration and proliferation may accelerate the wound healing process (Sung et al., 2020). The rate of cell migration was measured after disruption of the cell monolayer (Pitz et al., 2016). As shown in Fig. 6, AOM at both concentrations significantly increased the migration of L929 fibroblasts compared to the control group ($p < 0.05$). During the inicial 24 h period, AOM at 18.75 μg/mL and 37.50 μg/mL stimulated cell migration by 76.42 ± 4.24% and 79.93 ± 5.66%, respectively. A significant increase in cell migration rate was then observed after 48 h of treatment (97.86 ± 0.82% and 96.45 ± 1.96 for AOM at 18.75 μg/mL and 37.50 μg/mL, respectively). These results suggest that the extract is capable of enhancing cutaneous repair after injury, as they were significantly superior to those observed in the control group (24 h: 23.03 ± 1.72%; 48 h: 69.97 ± 3.90%) ($p < 0.05$).

According to Moro et al. (2021) results, the application of *A. oleracea* ointment to injured tendons of Lewis rats appeared to improve collagen synthesis and tendon repair compared to the control ($p < 0.0001$). These results can be attributed to the increased fibroblasts migration to the injury site, as these cells are responsible for collagen synthesis (Cañedo-Dorantes and Cañedo-Ayala, 2019; Moro et al., 2021). A study by Maria-Ferreira et al. (2018) also linked the *in vitro* wound-healing effect of *A. oleracea* leaves extracts to the rhamnogalacturonan polysaccharide. In comparison to the control, rhamnogalacturonan was able to accelerate wound closure of scratched Caco-2 cell monolayers by approximately 84% and 45% after 24 and 48 h, respectively ($p < 0.05$).

Our work reports for the first time the investigation and discussion of dermatological potential and wound healing properties of AOM. The *in vitro* wound healing activity of AOM may be related to the previously discussed anti-inflammatory and antioxidant potential of its bioactive compounds, which may stimulate fibroblast migration (Abdul-Rahim et al., 2021; Moro et al., 2021). Thus, our findings help to support the traditional use of Jambu for the treatment of skin and mucosal lesions, as well as infections and inflammatory conditions. (Araújo et al., 2021;

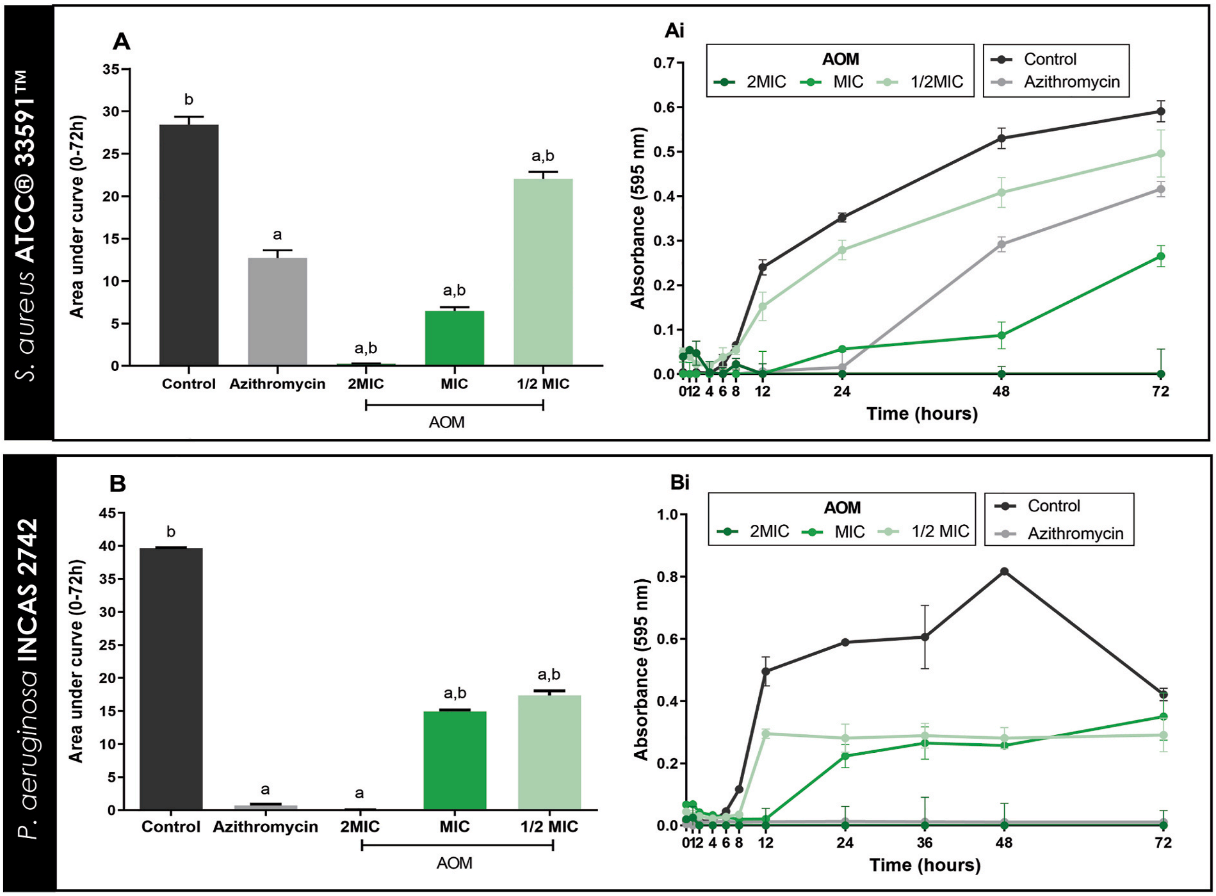

Fig. 4. Growth kinetics of *S. aureus* and *P. aeruginosa* treated with the methanolic extract from *A. oleracea* leaves (AOM) or azithromycin, used as a positive control. Bacterial species treated with AOM in different concentrations (2MIC, MIC, and ½ MIC values) or azithromycin (MIC value) were evaluated along 72 h of incubation. AOM vehicle served as control. (A) Area under the curve analyses (AUC) obtained from *S. aureus* growth kinetics. (Ai) *S. aureus* growth curve. (B) AUC analyses obtained from *P. aeruginosa* growth kinetics. (Bi) *P. aeruginosa* growth curve. a - Statistical difference from control (P < 0.05). b - Statistical difference from azithromycin (.). ANOVA followed by the Bonferroni test.

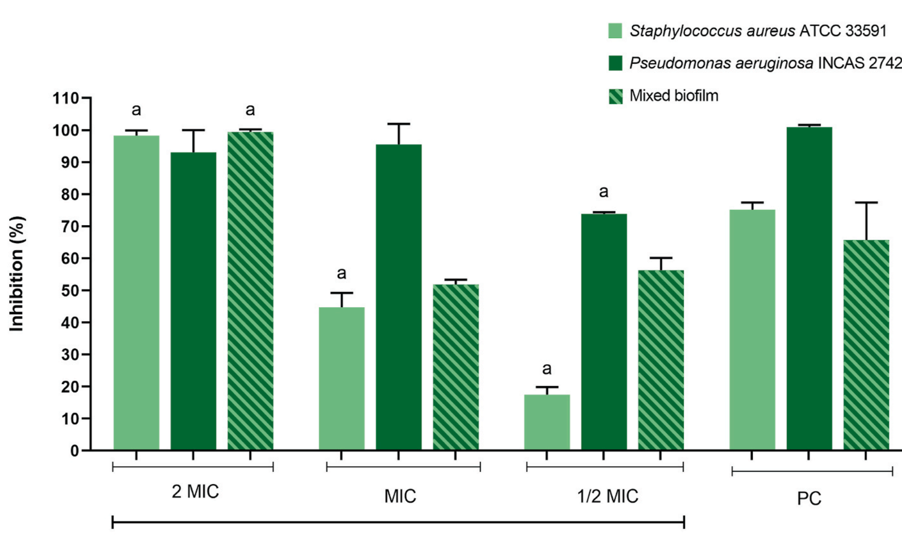

Fig. 5. Percentage of inhibition of *S. aureus*, *P aeruginosa,* and mixed biofilms treated with the methanolic extract from *A. oleracea* leaves (AOM) or azithromycin, used as a positive control (PC). *S. aureus* and *P. aeruginosa* were treated with AOM at 2MIC, MIC, and ½ MIC values or azithromycin at MIC value. Mixed cell suspensions were treated with AOM at *S. aureus* 2MIC, MIC, and ½ MIC values or azithromycin at *S. aureus* MIC value. a - Statistical difference from PC (P < 0.05). ANOVA followed by the Bonferroni test.

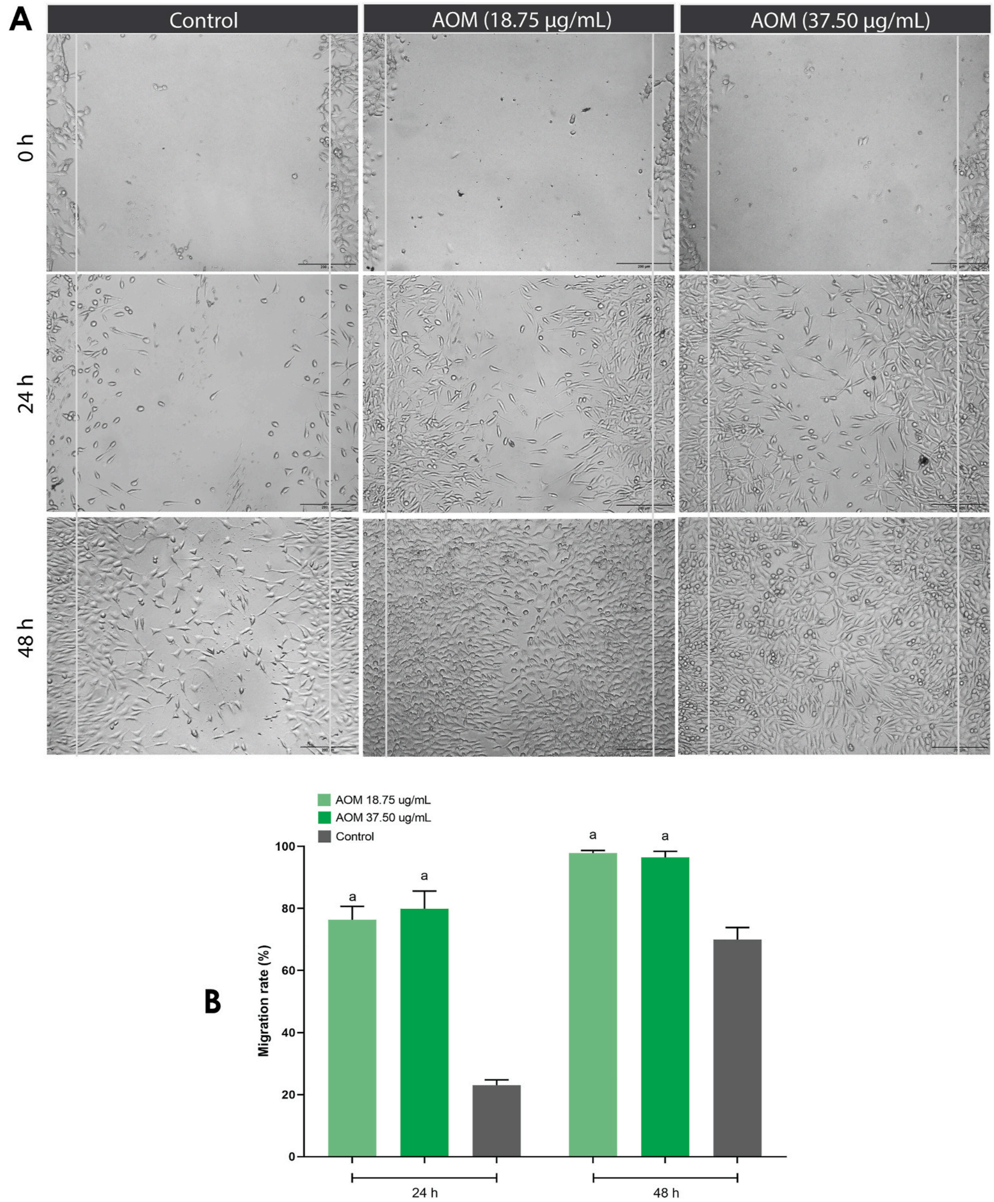

Fig. 6. Effect of the methanolic extract from *A. oleracea* leaves (AOM) on migration of L929 fibroblasts. (A) L299 fibroblasts treated with AOM (18.75 and 37.50 μg/mL) and control group at time 0, 24, and 48 h after scratching (scale bar: 200 μm). (B) L929 fibroblast migration rate 24 and 48 h after scratching. a - Statistical difference from control ($P < 0.05$). ANOVA followed by the Bonferroni test.

Bellumori et al., 2022).

4. Conclusion

This work reported the phytochemical composition of methanol extract from leaves of *Acmella oleracea* (AOM). Nine compounds, comprising alkylamides, including spilanthol and, phenolic molecules, as vanillic acid and quercetin, were identified in the AOM. The total antioxidant potential, anti-inflammatory, antimicrobial and wound healing activities of AOM is reported. AOM potently inhibited lipid peroxidation by 63,69 ± 3.47% and reduced cellular ROS production by 69.03 ± 3.85% demonstrating significant free radical scavenging activity. Furthermore, AOM suppressed cellular production of inflammatory mediators such as IL-6, TNF-α, NO and LDs by 100%, 96.66 ± 1.95%, 99.21 ± 3.82%, and 67.51 ± 0.72%, respectively. Additionally, AOM also showed significant antimicrobial activity against the major microorganisms commonly isolated from infected skin lesions. Adhesion of *S. aureus, P. aeruginosa* and mixed biofilms was significantly reduced by 44.71 ± 4.44%, 95.50 ± 6.37 %, and 51.83 ± 1.50%, respectively. Besides, the bacterial killing assay showed a reduction in the growth of *S. aureus* and *P. aeruginosa* by 77.17 ± 1.50% and 62.36 ± 1.01%, respectively. The extract also significantly enhanced the migration of L929 fibroblasts, suggesting a relevant wound healing activity. AOM may serve as a promising therapeutic alternative for wound treatment and may form the basis for future drug development. It also highlights the importance of this work in valuing Brazilian biodiversity, enabling the sustainable use of Amazonian resources and positively impacting the environment and local communities.

Funding

This work was supported by grants and scholarships from Conselho Nacional de Desenvolvimento Científico e Tecnológico (CNPq, Brazil - grant number: 408700/2021-1), Fundação de Amparo à Pesquisa do Estado de Minas Gerais (grant numbers: APQ-01357-21), Federal University of Juiz de Fora (UFJF/Brazil), and the Coordenação de

Aperfeiçoamento de Pessoal de Nível Superior (CAPES, Brazil). CNPq grants to R.L.F.

CRediT authorship contribution statement

Júlia Bertolini Fajardo: Writing – original draft, Methodology, Investigation, Conceptualization. **Mariana Hauck Vianna:** Methodology, Investigation. **Ana Barbara Polo:** Methodology, Investigation. **Mariane Rocha Cordeiro Comitre:** Methodology, Investigation. **Débora Almeida de Oliveira:** Methodology, Investigation. **Thayná Gomes Ferreira:** Methodology, Investigation. **Ari Sérgio de Oliveira Lemos:** Methodology, Investigation. **Thalita de Freitas Souza:** Methodology, Investigation. **Lara Melo Campos:** Writing – original draft, Methodology, Investigation. **Priscila de Lima Paula:** Writing – original draft, Methodology, Investigation. **Alan Franco Barbosa:** Resources, Investigation. **Mário Geraldo de Carvalho:** Writing – original draft, Methodology. **Maria Clara Machado Resende Guedes:** Methodology, Investigation. **Elaine Soares Coimbra:** Writing – original draft, Validation, Resources. **Gilson da Costa Macedo:** Writing – original draft, Resources, Funding acquisition. **Guilherme Diniz Tavares:** Writing – original draft, Resources. **Thaís Nogueira Barradas:** Writing – original draft, Supervision, Methodology, Investigation, Conceptualization. **Rodrigo Luiz Fabri:** Writing – review & editing, Writing – original draft, Supervision, Resources, Project administration, Funding acquisition, Formal analysis, Conceptualization.

Declaration of competing interest

The authors declare that they have no known competing financial interests or personal relationships that could have appeared to influence the work reported in this paper.

Data availability

No data was used for the research described in the article.

Acknowledgments

The authors thank Delfino Antonio Campos of the Department of Biochemistry, Federal University of Juiz de Fora, for technical assistance and Analytical Methods Platform of Farmanguinhos/FIOCRUZ by UFLC-QTOF-MS analysis.

References

Abdul-Rahim, R., Jayusman, P.A., Muhammad, N., Mohamed, N., Lim, V., Ahmad, N.H., Mohamad, S., Abdul Hamid, Z.A., Ahmad, F., Mokhtar, N., Shuid, A.N., 2021. Potential antioxidant and anti-inflammatory effects of *Spilanthes acmella* and its health beneficial effects: a review. Int. J. Environ. Res. Publ. Health 18, 3532. https://doi.org/10.3390/ijerph18073532.

Abeysiri, G.R.P.I., Dharmadasa, R.M., Abeysinghe, D.C., Samarasinghe, K., 2013. Screening of phytochemical, physico-chemical and bioactivity of different parts of *Acmella oleracea* Murr.(Asteraceae), a natural remedy for toothache. Ind. Crops Prod. 50, 852–856. https://doi.org/10.1016/j.indcrop.2013.08.043.

Abruzzo, A., Carola, P., Martina, R., Beatrice, V., Concettina, C., Federica, B., 2022. Development and characterization of azithromycin-loaded microemulsions: a promising tool for the treatment of bacterial skin infections. Antibiotics 11 (8), 1040. https://doi.org/10.3390/antibiotics11081040.

Araújo, C.A., Morgado, C.S., Gomes, A.K.C., Gomes, A.C.C., Simas, N.K., 2021. Asteraceae family: a review of its allelopathic potential and the case of *Acmella oleracea* and *Sphagneticola trilobata*. Rodriguesia 72, e01622020. https://doi.org/10.1590/2175-7860202172137.

Bakondi, E., Singh, S.B., Hajnády, Z., Nagy-Pénzes, M., Regdon, Z., Kovács, K., Hegedűs, C., Madácsy, T., Maléth, J., Hegyi, P., Demény, M.Á., Nagy, T., Keki, S., Szabó, É., Virág, L., 2019. Spilanthol inhibits inflammatory transcription factors and iNOS expression in macrophages and exerts anti-inflammatory effects in dermatitis and pancreatitis. Int. J. Mol. Sci. 20, 4308. https://doi.org/10.3390/ijms20174308.

Basselin, M., Robert-Gero, M., 1998. Alterations in membrane fuidity, lipid metabolism, mitochondrial activity, and lipophosphoglycan expression in pentamidine-resistant *Leishmania*. Parasitol. Res. 84, 78–83. https://doi.org/10.1007/s004360050361.

Bellumori, M., Zonfrillo, B., Maggini, V., Bogani, P., Gallo, E., Firenzuoli, F., Mulinacci, N., Innocenti, M., 2022. *Acmella oleracea* (L.) RK Jansen: alkylamides and phenolic compounds in aerial parts and roots of *in vitro* seedlings. J. Pharm. Biomed. Anal. 220, 114991. https://doi.org/10.1016/j.jpba.2022.114991.

Blanco, V.S.F., Michalak, B., Zelioli, Í.A.M., de Oliveira, A.D.S.S., Rodrigues, M.V.N., Ferreira, A.G., et al., 2018. Isolation of spilanthol from *Acmella oleracea* based on Green Chemistry and evaluation of its *in vitro* anti-inflammatory activity. J. Supercrit. Fluids 140, 372–379. https://doi.org/10.1016/j.supflu.2018.07.028.

Brand-Williams, W., Cuvelier, M.E., Berset, C., 1995. Use of a free radical method to evaluate antioxidant activity. LWT–Food Sci. Technol. 28, 25–30. https://doi.org/10.1016/S0023-6438(95)80008-5.

Bernatchez, S.F., Menon, V., Stoffel, J., Walters, S.A.H., Lindroos, W.E., Crossland, M.C., Shawler, L.G., Crossland, S.P., Boykin Jr., J.V., 2013. Nitric oxide levels in wound fluid may reflect the healing trajectory. Wound Repair Regen. 21, 410–417. https://doi.org/10.1111/wrr.12048.

Boonen, J., Bronselaer, A., Nielandt, J., Veryser, L., De Tre, G., Spiegeleer, B., 2012. Alkamid database: chemistry, occurrence and functionality of plant N-alkylamides. J. Ethnopharmacol. 142, 563–590. https://doi.org/10.1016/j.jep.2012.05.038.

Cañedo-Dorantes, L., Cañedo-Ayala, M., 2019. Skin acute wound healing: a comprehensive review. Int. J. Inflam. 3706315. https://doi.org/10.1155/2019/3706315.

Chin, J.S., Leigh, M., Sing, Y.C., David, L.B., 2019. Drug therapies and delivery mechanisms to treat perturbed skin wound healing. Adv. Drug Deliv. Rev. 149, 2–18. https://doi.org/10.1016/j.addr.2019.03.006.

Clinton, A., Carter, T., 2015. Chronic wound biofilms: pathogenesis and potential therapies. Lab. Med. 46, 277–284. https://doi.org/10.1309/LMBNSWKUI4JPN7SO.

Clinical and Laboratory Standards Institute (CLSI), 2020. Performance Standards for Antimicrobial Susceptibility Testing. M100, Wayne, USA.

Da Silva, C.A.P., Soares, C.P., Joaquim, W.M., Menegon, R.F., 2016. Mitochondrial activity and cell damage after application of *Acmella oleracea* leaf extract. Am. J. Plant Sci. 7 (17), 2498–2504. https://doi.org/10.4236/ajps.2016.717217.

Dallazen, J.L., Maria-Ferreira, D., da Luz, B.B., Nascimento, A.M., Cipriani, T.R., de Souza, L.M., Felipe, L.P.G., Silva, B.J.G., Nassini, R., Werner, M.F.P., 2020. Pharmacological potential of alkylamides from *Acmella oleracea* flowers and synthetic isobutylalkyl amide to treat inflammatory pain. Inflammopharmacology 28, 175–186. https://doi.org/10.1007/s10787-019-00601-9.

Dehdashtian, A., Stringer, T.P., Warren, A.J., Mu, E.W., Amirlak, B., Shahabi, L., 2018. Anatomy and physiology of the skin. In: Melanoma: A Modern Multidisciplinary Approach. Springer Int Publish, pp. 15–26. https://doi.org/10.1007/978-3-319-78310-9_2.

Dunnill, C., Patton, T., Brennan, J., Barrett, J., Dryden, M., Cooke, J., Leaper, D., Georgopoulos, N.T., 2017. Reactive oxygen species (ROS) and wound healing: the functional role of ROS and emerging ROS-modulating technologies for augmentation of the healing process. Int. Wound J. 14, 89–96. https://doi.org/10.1111/iwj.12557.

Elbadrawy, E., Sello, A., 2016. Evaluation of nutritional value and antioxidant activity of tomato peel extracts. Arab. J. Chem. 9, S1010–S1018. https://doi.org/10.1016/j.arabjc.2011.11.011.

Elufioye, T.O., Habtemariam, S., Adejare, A., 2020. Chemistry and pharmacology of alkylamides from natural origin. Rev. Bras. Farmacogn. 30, 622–640. https://doi.org/10.1007/s43450-020-00095-5.

Fabri, R.L., Freitas, J.C., Lemos, A.S., Campos, L.M., Diniz, I.O., Pinto, N.C., Silva, T.P., Palazzi, C., Marchesini, P., Monteiro, C., Barbosa, A.F., 2021. Spilanthol as a promising antifungal alkylamide for the treatment of vulvovaginal candidiasis. Med. Mycol. 59, 1210–1224. https://doi.org/10.1093/mmy/myab054.

Folin, O., Ciocalteu, V., 1927. On tyrosine and tryptophane determinations in proteins. J. Biol. Chem. 73, 627–650. https://doi.org/10.1016/S0021-9258(18)84277-6.

Gay, N.H., Phopin, K., Suwanjang, W., Songtawee, N., Ruankham, W., Wongchitrat, P., Prachayasittikul, S., Prachayasittikul, V., 2018. Neuroprotective effects of phenolic and carboxylic acids on oxidative stress-induced toxicity in human neuroblastoma SH-SY5Y cells. Neurochem. Res. 43, 619–636. https://doi.org/10.1007/s11064-017-2463-x.

Gilbert, B., Favoreto, R., 2010. *Acmella oleracea* (L.) RK jansen (Asteraceae) jambu. Ver. Fitos. 5, 83–91. https://www.arca.fiocruz.br/handle/icict/15932.

Gonçalves, A.E., Silveira, N., de Oliveira, L., Lima, M.G., Biavatti, M., Cazarin, C., Souza, M., 2021. Protective effect of acmella ciliata extract and spilanthol in streptozotocin-induced sporadic alzheimer's disease mouse model: possible involvement of the of decreased oxidative stress by activating TRPV1 receptors. https://doi.org/10.21203/rs.3.rs-282279/v1.

Grand View Research, 2023. Wound care market size, share & trends analysis by product (advanced, traditional), by application (chronic wounds), by end-use (hospitals, nursing homes), by mode of purchase, by distribution channel, by region, and segment forecasts, 2024 – 2030. https://www.grandviewresearch.com/industry-analysis/wound-care-market.

Gushiken, L.F.S., Beserra, F.P., Bastos, J.K., Jackson, C.J., Pellizzon, C.H., 2021. Cutaneous wound healing: an update from physiopathology to current therapies. Life 11, 665. https://doi.org/10.3390/life11070665.

Huang, C.H., Chang, L.C., Hu, S., Hsiao, C.Y., Wu, S.J., 2018. Spilanthol inhibits TNF-α-induced ICAM-1 expression and pro-inflammatory responses by inducing heme oxygenase-1 expression and suppressing pJNK in HaCaT keratinocytes. Mol. Med. Rep. 18 (3), 2987–2994. https://doi.org/10.3892/mmr.2018.9245.

Jin, H.J., Lee, J., Kim, D.H., Kim, K.T., 2015. Antioxidative and nitric oxide scavenging activity of branched-chain amino acids. Food Sci. Biotechnol. 24, 1555–1558. https://doi.org/10.1007/s10068-015-0200-2.

Kim, K.H., Kim, E.J., Kwun, M.J., Lee, J.Y., Bach, T.T., Eum, S.M., Joo, M., 2018. Suppression of lung inflammation by the methanol extract of *Spilanthes acmella* Murray is related to differential regulation of NF-κB and Nrf2. J. Ethnopharmacol. 217, 89–97. https://doi.org/10.1016/j.jep.2018.02.011.

Lalthanpuii, P.B., Hruaitluangi, L., Sailo, N., Lalchhandama, H.T., 2017. Nutritive value and antioxidant activity of *Acmella oleracea* (Asteraceae), a variety grown in Mizoram, India. Int. J. Phytopharm. 7, 42–46. https://doi.org/10.7439/ijpp.v7i5.4385.

Lalthanpuii, P.B., Lalawmpuii, R., Lalremsanga, H.T., Lalchhandama, K., 2018. Pharmacognostic study of the medicinal plant *Acmella oleracea*: analysis of its chemical components and properties. Biodivers. Conserv.: Strategies and Appçications 303–313. ISBN 978-81-937-3274-8.

Larouche, J., Sheoran, S., Maruyama, K., Martino, M.M., 2018. Immune regulation of skin wound healing: mechanisms and novel therapeutic targets. Adv. Wound Care 7, 209–231. https://doi.org/10.1089/wound.2017.0761.

Lemos, A.S.O., Florêncio, J.R., Pinto, N.C.C., Campos, L.M., Silva, T.P., Grazul, R.M., Pinto, P.F., Tavares, G.D., Scio, E., Apolônio, A.C.M., Melo, R.C.N., Fabri, R.L., 2020. Antifungal activity of the natural coumarin scopoletin against planktonic cells and biofilms from a multidrug-resistant *Candida tropicalis* strain. Front. Microbiol. 11, 1525. https://doi.org/10.3389/fmicb.2020.01525.

Man, M.Q., Wakefield, J.S., Mauro, T.M., Elias, P.M., 2022. Regulatory role of nitric oxide in cutaneous inflammation. Inflammation 45, 1–16. https://doi.org/10.1007/s10753-021-01615-8.

Melo, R.C., Weller, P.F., 2016. Lipid droplets in leukocytes: organelles linked to inflammatory responses. Exp. Cell Res. 340, 193–197. https://doi.org/10.1016/j.yexcr.2015.10.028.

Maria-Ferreira, D., Nascimento, A.M., Cipriani, T.R., Santana-Filho, A.P., Watanabe, P.D. S., Sant' Ana, D.D.M.G., Luciano, F.B., Bocate, K.C.P., Wijngaard, R.M., Werner, M.F. P., Baggio, C.H., 2018. Rhamnogalacturonan, a chemically-defined polysaccharide, improves intestinal barrier function in DSS-induced colitis in mice and human Caco-2 cells. Sci. Rep. 8 (1), 12261. https://doi.org/10.1038/s41598-018-30526-2.

Maver, T., Maver, U., Stana Kleinschek, K., Smrke, D.M., Kreft, S., 2015. A review of herbal medicines in wound healing. Int. J. Dermatol. 54, 740–751. https://doi.org/10.1111/ijd.12766.

Meerwein, M., Tarnutzer, A., Böni, M., Van Bambeke, F., Hombach, M., Zinkernagel, A. S., 2020. Increased azithromycin susceptibility of multidrug-resistant gram-negative bacteria on RPMI-1640 agar assessed by disk diffusion testing. Antibiotics 9 (5), 218. https://doi.org/10.3390/antibiotics9050218.

Moro, S.D.D.S., de Oliveira Fujii, L., Teodoro, L.F.R., Frauz, K., Mazoni, A.F., Esquisatto, M.A.M., Rodrigues, R.A.F., Pimentel, E.R., de Aro, A.A., 2021. *Acmella oleracea* extract increases collagen content and organization in partially transected tendons. MRT 84 (11), 2588–2597. https://doi.org/10.1002/jemt.23809.

Mosmann, T., 1983. Rapid colorimetric assay for cellular growth and survival: application to proliferation and cytotoxicity assays. J. Immunol. Methods 65, 55–63. https://doi.org/10.1016/0022-1759(83)90303-4.

Murthy, H.N., Kee-Yoeup, P., 2021. Bioactive Compounds in Underutilized Vegetables and Legumes, vol. 87. Springer. ISBN-10: 3030574164.

Nabi, N.G., Shrivastava, M., 2016. Estimation of total flavonoids and antioxidant activity of *Spilanthes acmella* leaves. Pharmeuropa Bio J. 4 (29). https://doi.org/10.20510/ukjpb/4/i6/134657.

Nascimento, L.E.S., Arriola, N.D.A., Da Silva, L.A.L., Faqueti, L.G., Sandjo, L.P., De Araújo, C.E.S., Biavatti, M.W., Barcelos-Oliveira, J.L., Amboni, R.D.D.M.C., 2020. Phytochemical profile of different anatomical parts of jambu (*Acmella oleracea* (L.) RK Jansen): a comparison between hydroponic and conventional cultivation using PCA and cluster analysis. Food Chem. 332, 127393. https://doi.org/10.1016/j.foodchem.2020.127393.

Nipate, S.S., Tiwari, A.H., 2020. Antioxidant and immunomodulatory properties of Spilanthes oleracea with potential effect in chronic fatigue syndrome infirmity. J-AIM 11 (2), 124–130. https://doi.org/10.1016/j.jaim.2017.08.008.

Osawa, C.C., Felício, P.E., Gonçalves, L.A.G., 2005. Teste de TBA aplicado a carnes e derivados: métodos tradicionais, modificados e alternativos. Quim. Nova 28, 655–663. https://doi.org/10.1590/S0100-40422005000400019.

Patel, R.M., Patel, N.J., 2011. *In vitro* antioxidant activity of coumarin compounds by DPPH, Super oxide and nitric oxide free radical scavenging methods. J. Adv. Pharm. Educ. Res. 1, 52–68.

Pereira, L.O.M., Vilegas, W., Tangerina, M.M.P., Arunachalam, K., Balogun, S.O., Orlandi-Mattos, P.E., Colodel, E.M., de Oliveira Martins, D.T., 2018. Lafoensia pacari A. St.-Hil.: wound healing activity and mechanism of action of standardized hydroethanolic leaves extract. J. Ethnopharmacol. 219, 337–350. https://doi.org/10.1016/j.jep.2018.02.038.

Peretti, P., Rodrigues, E.T., De Souza Junior, B.M., Bezerra, R.M., Fernandez, E.G., De Sousa, F.F.O., Pinheiro, M.T., 2021. Spilanthol content of *Acmella oleracea* subtypes and their bactericide and antibiofilm activities against *Streptococcus mutans*. South Afr. J. Bot. 143, 17–24. https://doi.org/10.1016/j.sajb.2021.08.001.

Petkovic, M., Mouritzen, M.V., Mojsoska, B., Jenssen, H., 2021. Immunomodulatory properties of host defence peptides in skin wound healing. Biomol 11, 952. https://doi.org/10.3390/biom11070952.

Pitz, H.D.S., Pereira, A., Blasius, M.B., Voytena, A.P.L., Affonso, R.C., Fanan, S., Trevisan, A.C.D., Ribeiro-do-Valle, R.M., Maraschin, M., 2016. *In vitro* evaluation of the antioxidant activity and wound healing properties of Jaboticaba (Plinia peruviana) fruit peel hydroalcoholic extract. Oxid. Med. Cell. Longev. 2016 (1), 3403586. https://doi.org/10.1155/2016/3403586.

Prieto, P., Pineda, M., Aguilar, M., 1999. Spectrophotometric quantitation of antioxidant capacity through the formation of a phosphomolybdenum complex: specific application to the determination of vitamin E. Anal. Biochem. 269, 337–341. https://doi.org/10.1006/abio.1999.4019.

Sadan, H., Shanthala, B.M., Zareena, M.A., Babu, G., Vijayan, V., 2020. *In vitro* evaluation of milk-based, soy-based, and amino acid-based infant formulas on *Streptococcus mutans* biofilm formation. J. Indian Soc. Pedod. Prev. Dent. 38, 350–354. https://doi.org/10.4103/JISPPD.JISPPD_241_20.

Santos-sánchez, N.F., Salas-Coronado, R., Villanueva-Cañongo, C., Hernández-Carlos, B., 2019. Antioxidant compounds and their antioxidant mechanism. Antioxidants 10, 1–29. https://doi.org/10.5772/intechopen.85270.

Savic, S., Petrovic, S., Savic, S., Cekic, N., 2021. Identification and photostability of N-alkylamides from *Acmella oleracea* extract. J. Pharm. Biomed. Anal. 195, 113819. https://doi.org/10.1016/j.jpba.2020.113819.

Sharma, R., Arumugam, N., 2021. N-alkylamides of *Spilanthes* (syn: *acmella*): structure, purification, characterization, biological activities and applications–a review. Future Foods 3, 100022. https://doi.org/10.1016/j.fufo.2021.100022.

Shukla, S.K., Sharma, A.K., Gupta, V., Yashavarddhan, M.H., 2019. Pharmacological control of inflammation in wound healing. J. Tissue Viability 28, 218–222. https://doi.org/10.1016/j.jtv.2019.09.002.

Silva, S.P., Fernandes, J.A.L., Santos, A.S., Ferreira, N.R., 2023. Jambu flower extract (*Acmella oleracea*) increases the antioxidant potential of beer with a reduced alcohol content. Plants 12, 1581. https://doi.org/10.3390/plants12081581.

Simões, D., Miguel, S.P., Ribeiro, M.P., Coutinho, P., Mendonça, A.G., Correia, I.J., 2018. Recent advances on antimicrobial wound dressing: a review. Eur. J. Pharm. Biopharm. 127, 130–141. https://doi.org/10.1016/j.ejpb.2018.02.022.

Stein, R., Berger, M., de Cecco, B.S., Mallmann, L.P., Terraciano, P.B., Driemeier, D., Rodrigues, E., Beys-da-Silva, W.O., Konrath, E.L., 2021. Chymase inhibition: a key factor in the anti-inflammatory activity of ethanolic extracts and spilanthol isolated from *Acmella oleracea*. J. Ethnopharmacol. 270, 113610. https://doi.org/10.1016/j.jep.2020.113610.

Stroppa, P.H.F., Antinarelli, L.M.R., Carmo, A.M.L., Gameiro, J., Coimbra, E.S., da Silva, A.D., 2017. Effect of 1,2,3-triazole salts, non-classical bioisosteres of miltefosine, on *Leishmania amazonenses*. Bioorg. Med. Chem. 25, 3034–3045. https://doi.org/10.1016/j.bmc.2017.03.051.

Sun, J., Zhang, X., Broderick, M., Fein, H., 2003. Measurement of nitric oxide production in biological systems by using griess reaction assay. Sensors 3, 276–284. https://doi.org/10.3390/s30800276.

Sung, T.J., Wang, Y.Y., Liu, K.L., Chou, C.H., Lai, P.S., Hsieh, C.W., 2020. Pholiota nameko polysaccharides promotes cell proliferation and migration and reduces ROS content in H2O2-induced L929 cells. Antioxidants 9 (1), 65. https://doi.org/10.3390/antiox9010065.

Suriyaprom, S., Mosoni, P., Leroy, S., Kaewkod, T., Desvaux, M., Tragoolpua, Y., 2022. Antioxidants of fruit extracts as antimicrobial agents against pathogenic bacteria. Antioxidants 11 (602). https://doi.org/10.3390/antiox11030602.

Thakur, S., Sagar, A., Prakash, V., 2019. Studies on antibacterial and antioxidant activity of different extracts of *Spilanthes acmella* L. Plant. Arch. 19, 1711–1717 e-ISSN:2581-6063/ISSN:0972-5210.

Thonemann, B., Schmals, G., Hiller, K.A., Schweik, 2002. Responses of L929 mouse fibroblasts, primary and immortalized bovine dental papilla-derived cell lines to dental resin components. Dent. Mater. 18, 318–323. https://doi.org/10.1016/s0109-5641(01)00056-2.

Uthpala, T.G.G., Navaratne, S.B., 2021. *Acmella oleracea* plant; identification, applications and use as an emerging food source - review. Food Rev. Int. 37, 399–414. https://doi.org/10.1080/87559129.2019.1709201.

Visha, M.G., Karunagaran, M., 2019. A review on wound healing. Int. J. Clinicopathological Correl. 3, 50–59. https://doi.org/10.4103/ijcpc.ijcpc_13_19.

Yadav, U.C.S., Ramana, K.V., 2013. Regulation of NF-kB-Induced inflammatory signaling by lipid peroxidation-derived aldehydes. Oxid. Med. Cell. Longev. 2013, 1–11. https://doi.org/10.1155/2013/690545.

Yazarlu, O., Iranshahi, M., Kashani, H.R.K., Reshadat, S., Habtemariam, S., Iranshahy, M., Hasanpour, M., 2021. Perspective on the application of medicinal plants and natural products in wound healing: a mechanistic review. Pharmacol. Res. 174. https://doi.org/10.1016/j.phrs.2021.105841.

Zhou, Y., Liu, M.J., Liao, X.Y., Chen, Y.T., Liao, Q.X., Lin, J.D., Lin, H.R., Huang, Y.H., 2023. New attempts to inhibit methicillin-resistant Staphylococcus aureus biofilm? A combination of daptomycin and azithromycin. Infect. Drug Resist. 16, 7029–7040. https://10.2147/IDR.S433439.